Concerted expression of a cell cycle regulator and a metabolic enzyme from a bicistronic transcript in plants

Lorenzo-Orts, Laura; Witthoeft, Janika; Deforges, Jules; Martinez Font, Jacobo; Loubery, Sylvain Philippe; Placzek, Aleksandra; Poirier, Yves; Hothorn, Ludwig A.; Jaillais, Yvon; Hothorn, Michael

How to cite

LORENZO-ORTS, Laura et al. Concerted expression of a cell cycle regulator and a metabolic enzyme from a bicistronic transcript in plants. In: Nature Plants, 2019, vol. 5, n° 2, p. 184–193. doi: 10.1038/s41477-019-0358-3

This publication URL: https://archive-ouverte.unige.ch/unige:121410
Publication DOI: 10.1038/s41477-019-0358-3

Concerted expression of a cell-cycle regulator and a metabolic enzyme from a bicistronic transcript in plants.

Laura Lorenzo-Orts[1,$], Janika Witthoeft[2], Jules Deforges[3], Jacobo Martinez[1,2], Sylvain Loubéry[4], Aleksandra Placzek[2,+], Yves Poirier[3], Ludwig A. Hothorn[5,#], Yvon Jaillais[6], Michael Hothorn[1,2,$]

[1]Structural Plant Biology Laboratory, Department of Botany and Plant Biology, University of Geneva, Geneva, Switzerland.

[2]Friedrich Miescher Laboratory of the Max Planck Society, Tübingen, Germany

[3]Department of Plant Molecular Biology, University of Lausanne, Lausanne, Switzerland

[4]Department of Botany and Plant Biology, University of Geneva, Geneva, Switzerland.

[5]Institute of Biostatistics, Leibniz University, Hannover, Germany.

[6]Laboratoire Reproduction et Développement des Plantes, Université de Lyon, ENS de Lyon, UCB Lyon 1, CNRS, INRA, F-69342 Lyon, France.

[+]Present address: Max Planck Institute for Biology of Ageing, Cologne, Germany.

[#]retired

[$]correspondence: laura.lorenzo@unige.ch, michael.hothorn@unige.ch

Abstract

Eukaryotic mRNAs frequently contain upstream open reading frames (uORFs), encoding small peptides which may control translation of the main ORF (mORF). Here we report the characterization of a distinct bicistronic transcript in Arabidopsis. We analyzed loss-of-function phenotypes of the inorganic polyphosphatase AtTTM3, and found that catalytically inactive versions of the enzyme could fully complement embryo

and growth-related phenotypes. We could rationalize these puzzling findings by characterizing a uORF in the AtTTM3 locus encoding an ortholog of the cell cycle regulator CDC26. We demonstrate that AtCDC26 is part of the plant anaphase promoting complex/cyclosome (APC/C), regulates accumulation of APC/C target proteins and controls cell division, growth and embryo development. AtCDC26 and AtTTM3 are translated from a single transcript conserved across the plant lineage. While there is no apparent biochemical connection between the two gene products, AtTTM3 coordinates AtCDC26 translation by recruiting the transcript into polysomes. Our work highlights that uORFs may encode functional proteins in plant genomes.

Introduction

uORFs are coding sequences in the 5' untranslated region (UTR) of mRNAs. Many uORFs code for small, non-conserved peptides[1,2] and regulate expression of the mORF[3]. While a significant fraction of fungal, animal and plant genes contain uORFs[4], only few uORF-derived peptides have been found in cells and tissues[1,5]. In plants, several uORFs have been genetically characterized in transcription factors, metabolic enzymes, membrane transporters and signaling proteins[6]. uORFs regulate the expression of the mORF during growth and development[7,8], in response to stress[9,10] or to changes in sucrose availability[11]. As in other eukaryotes, plant uORFs can be involved in translational repression of the mORF[8] and in the nonsense mediated decay (NMD) of the respective mRNA[12–14].

Independent, functional proteins can be transcribed together from *bona fide* bi- or polycistronic transcripts[15,16]. Eukaryotic transcripts encoding for more than one protein have been initially reported from vertebrates, where the transforming growth factor-beta family ligand GDF1 is transcribed together with ceramide synthase 1 from a single 3 kb transcript[17].

Other examples include the p16^{INK4a} gene, which contains two overlapping open reading frames coding for distinct proteins involved in cell cycle regulation[18]. A similar gene architecture has been reported for the mammalian XLαs/Gαs gene. Here, the two translation products code for the extra-large G-protein XLαs and for a sequence-unrelated protein ALEX, which directly binds XLαs[19]. A uORF located in the mammalian A_{2A} adenosine G-protein coupled receptor gene encodes the ~ 15 kDa uORF5 protein, whose expression is regulated by A_{2A} activation[20]. These examples may suggest that mORF and uORF protein products are often functionally and/or biochemically linked[15], but mORF/uORF pairs with no apparent biological connection have been described as well[21].

Results

Here we report a novel uORF with unusual properties located in the annotated 5' UTR of *TTM3* (At2g11890) in Arabidopsis. *AtTTM3* encodes an inorganic polyphosphatase that releases inorganic phosphate from short-chain linear polyphosphates, a storage form of phosphate in many pro- and eukaryotes[22,23]. *TTM3* is a conserved single copy gene in Arabidopsis and many other plant species (Supplementary Fig. 1). To define physiological functions for TTM3, we analyzed different *ttm3* mutant alleles: *ttm3-1* maps to the *TTM3* ORF (Fig. 1a), completely abolishes TTM3 expression and protein accumulation (Fig. 1b) and reduces hypocotyl and root growth, in agreement with an earlier report[22] (Fig. 1d, e). A second T-DNA insertion in the 5' UTR of *TTM3* (*ttm3-2*) likely causes a knock-out of TTM3, impairs embryo development and blocks seed germination (Fig. 1c, 3d). *ttm3-4* maps to the 3' UTR, shows reduced TTM3 transcript and protein levels (Fig. 1b) and displays a weak growth phenotype (Fig. 1d,e). The observed inconsistencies between the *ttm3-1* and *ttm3-2* mutant lines prompted us to generate an additional CRISPR/Cas9-based mutant. The resulting *ttm3-3* allele harbors a 16 base-pair deletion in the *TTM3* coding sequence

(Supplementary Fig. 1) that abolishes TTM3 protein accumulation and also reduces *TTM3* transcript levels *in planta* (Fig. 1b). To our surprise, *ttm3-3* mutants did neither resemble the root and hypocotyl growth phenotypes of *ttm3-1* plants nor the *ttm3-2* embryo phenotype (Fig. 1d, e).

We investigated these phenotypic differences by complementing *ttm3-1* and *ttm3-2* mutant alleles with the fluorescent protein-tagged TTM3-mCITRINE expressed under the control of the *TTM3* promoter, including the annotated 5' UTR. Even though TTM3-mCITRINE protein levels were low compared to endogenous TTM3, we observed full complementation of the different *ttm3* alleles, suggesting that the observed phenotypes were specific to the *TTM3* locus (Fig. 2a, b). We analyzed TTM3-mCITRINE and TTM3-GUS transgenic reporter lines and found that TTM3 is a cytoplasmic/nuclear localized protein expressed in ovules, roots and hypocotyls, in good agreement with the observed phenotypes (Supplementary Fig. 2). We next complemented the embryo phenotype of *ttm3-2* plants with versions of TTM3 compromised in either substrate binding or catalysis[23] (Fig. 2c). To our surprise, catalytically inactive versions of TTM3 could fully complement the *ttm3-2* mutant phenotype (Fig. 2d, e), indicating that the enzymatic activity of TTM3 is dispensable for proper embryo development.

Close inspection of the *TTM3* locus revealed the presence of a putative uORF in the annotated 5'UTR of TTM3, ending 8 base-pairs upstream of the mORF start codon (Fig. 3a, Supplementary Fig. 3). The uORF encodes a hypothetical protein of 65 amino acids, sharing significant sequence homology with CDC26 super-family proteins, as previously proposed by Vaughn *et al*.[24] (Fig. 3a). CDC26, whose genome locus was previously unknown[25,26], forms a component of the APC/C, an E3-ubiquitin ligase that targets substrates for degradation, allowing for cell cycle progression[27]. AtCDC26 protein accumulates in different plant tissues

throughout development (Fig. 3b). Since *ttm3* phenotypes did not seem to be related to TTM3 protein levels or its catalytic activity, we analyzed AtCDC26 transcript and protein expression levels in *ttm3-1*, *ttm3-3* and *ttm3-4* mutants. Although transcript levels were lower, we found no observable differences for AtCDC26 protein levels in the non-lethal *ttm3-1*, *ttm3-3* and *ttm3-4* mutants (Fig. 3c).

Based on these observations, we hypothesized that complementation of our *ttm3-1* and *ttm3-2* mutant lines (Fig. 2a-d) may have been due to the re-introduction of functional AtCDC26, present in what we thought would be the *TTM3* 5' UTR. We could indeed detect wild-type levels of AtCDC26 in our *ttm3-2* complemented lines (Fig. 2f). Ubiquitous expression of the AtCDC26 CDS alone fully rescued *ttm3-2* embryo lethality and *ttm3-1* defective root and hypocotyl growth (Fig. 3d-f), suggesting that the observed and reported[22] phenotypes for *ttm3-1* were caused by interference with *CDC26* expression, rather than *TTM3* loss-of-function.

We next tested if AtCDC26 is a *bona fide* component of the Arabidopsis APC/C. We performed immunoprecipitation assays followed by mass-spectrometry in wild-type plants expressing epitope-tagged AtCDC26-6xHA. AtCDC26 interactors included APC1, APC5, APC6 and APC3/CDC27B, which have been previously shown to interact with CDC26 in human[28], and in addition APC2 and APC8, together forming the APC/C complex (Fig. 3g)[27,29]. The plant APC/C regulates cell division and affects many aspects of plant growth and development[25,30]. To test whether *ttm3-1* mutant plants have abnormal cell divisions cycles, we quantified GFP levels in *ttm3-1* plants expressing fluorescent tagged Cyclin B1;1 (CYCB1;1-GFP[31]). CYCB1;1 is a marker of cell division and a target of the APC/C[32,33]. We found that CYCB1;1-GFP expression and protein levels (inferred from the GFP fluorescent signal) are less variable and overall reduced in *ttm3-1* plants vs. wild-type plants, indicating

that the mutant is defective in cell division and CYCB1;1-GFP protein stability, respectively (Fig. 3h). Together, our findings suggest that AtCDC26 is a plant cell-cycle regulator and part of the Arabidopsis APC/C. Importantly, we did not recover TTM3 peptides in our immunoprecipitation assays and recombinant AtTTM3 and AtCDC26 showed no detectable interaction in *in vitro* isothermal titration calorimetry assays, suggesting that TTM3 does not form part of the plant APC/C complex (Supplementary Fig. 4).

CDC26 and *TTM3* are both present in the entire plant lineage and their ORFs are always in close proximity (Fig. 4a, Supplementary Fig. 3)[24]. The *CDC26* stop codon may be spaced ~150 base-pairs apart from the start codon of *TTM3* (e.g. in *Chlamydomonas reinhardtii* and *Marchantia polymorpha*), be separated by only a short stretch (in Arabidopsis), or the ORFs may even overlap, as found for example in tomato and maize (Fig. 4a, Supplementary Fig. 3). As *CDC26* and *TTM3* are always in close proximity, we speculated that both proteins could be expressed from a single bicistronic transcript. We performed northern blots with probes against *CDC26* and *TTM3* in wild-type and *ttm3-1* mutant plants. We detected a major transcript of ~1,200 nucleotides using both probes, which is absent in *ttm3-1* plants (Fig. 4b). Next, we performed 5' and 3' RACE experiments with *CDC26* specific primers and recovered a transcript of similar size (Fig. 4c). Sequencing of 5' RACE products confirmed the presence of the *CDC26* and *TTM3* ORFs in a single transcript in wild-type plants (see Supplementary Information). One additional transcript was recovered in the RACE experiments, encoding CDC26 only (see Supplementary Information). The presence of both transcripts could be confirmed in RT-PCR experiments (Fig. 4d). Previously reported cDNA clones suggest that *CDC26* and *TTM3* are encoded in a single transcript in Chlamydomonas, tomato and maize (Supplementary Fig. 3). To test if AtCDC26 and AtTTM3 are translated from a single mRNA, we performed *in vitro* translation assays in wheat germ extracts, where

products were labeled with ^{35}S methionine. Two protein products migrating at the expected size of AtCDC26 and AtTTM3, respectively, were produced from an *in vitro* transcribed *CDC26-TTM3* transcript (Fig. 4e). Mutating the start codon of either *CDC26* or *TTM3* eliminated translation of the respective gene product, but did not affect translation of the other ORF (Fig. 4e). Together our *in vivo* and *in vitro* experiments reveal that CDC26 and TTM3 are transcribed and translated from a single transcript, yielding two proteins with different biochemical and physiological functions. The *ttm3-3* allele and the complementation experiments using catalytically inactive versions of TTM3 together suggest that neither the enzyme itself nor its catalytic function impact the phenotypes described for the *TTM3* locus[22].

Our loss-of-function phenotypes reveal an essential role for CDC26 in Arabidopis, as previously seen in animals[34]. The *CDC26* transcript contains a long second ORF encoding TTM3 in its 3' region. The fact that this bicistronic configuration is conserved in the plant lineage suggests that it may have regulatory functions in plant cell cycle control. Translation of different cyclin-dependent kinases from a single transcript occurs via cell-cycle regulated internal ribosome entry sites (IRES) in metazoa[35], but this mechanism may not be wide-spread in plants[6]. Notably, expression of AtCDC26 from a strong ubiquitous promoter alone can rescue all observed phenotypes, while expression of AtCDC26 under control of its native promoter requires the endogenous 3'UTR or the presence of the *TTM3* mORF (Supplementary Fig. 5). Complementation of a *ttm3-2* mutant with a construct harboring a mutated CDC26 start codon (*CDC26-TTM3) did not rescue the *ttm3-2* embryo lethal phenotype (Fig. 5a,b). In contrast, we observed stunted-growth and 'broom-head' phenotypes previously seen in *APC6* and *APC10* knock-down mutants[36] or in a *APC8* missense allele[37], when complementing *ttm3-2* plants with a construct harboring a mutated *TTM3* start codon (CDC26-*TTM3) (Fig. 5a,c). *CDC26* transcript levels are high in plants expressing CDC26-

*TTM3 but protein levels were reduced compared to wild-type, indicating that CDC26 and TTM3 may require to be translated in a concerted fashion (Fig. 5d). To investigate this issue further, we performed polysome profiling experiments. We found the *TTM3* transcript associated with polysomes in wild-type seedlings, but to a lesser extend in CDC26-*TTM3 plants, indicating that TTM3 translation recruits the biscistronic transcript to polysomes (Fig. 5e).

It has been previously reported that the Target Of Rapamycin (TOR) complex can regulate uORF translation and loading of the respective transcripts to polysomes[7,38]. We thus tested whether CDC26 and TTM3 expression is regulated by TOR. In agreement with a previous study[7], the uORF-containing transcript *bZIP11* tends to be shifted to monosomes upon treatment with the TOR-inhibitor AZD8055 (AZD), while the polysome profile of *TTM3* seems unaffected (Supplementary Fig. 6). In line with this, TTM3 and CDC26 protein levels are not significantly reduced in seedlings treated with the TOR-inhibitors KU63794 (KU) and AZD8055 (AZD), when compared to the actin loading control (Supplementary Fig. 6). These experiments together indicate that TOR may not have a major role in the translational regulation of CDC26 and TTM3.

Finally, we tested if the *CDC26-TTM3* transcript is regulated by NMD, as previously reported for other uORF containing transcripts in Arabidopsis[12–14]. We found *CDC26-TTM3* transcript levels to be higher in wild-type plants treated with cycloheximide (CHX), an inhibitor of protein translation that represses NMD[39] (Fig. 6a), or in known NMD mutant backgrounds (Fig. 6b). Consistently, also CDC26 and TTM3 protein levels were increased in NMD mutants (Fig. 6c). Together, these experiments indicate that the *CDC26-TTM3* bicistronic transcript is regulated by nonsense-mediated decay.

Discussion

In Arabidopsis, uORF-containing mRNAs represent more than 30% of the transcriptome and these uORFs may control translation efficiency and mRNA stability of the mORF[6]. It has been proposed that several 'large' uORFs (100-250 base-pairs) may exist in plants, possibly encoding functional proteins[24]. Here we characterize one of them, the uORF associated with At2g11890. We demonstrate that this uORF encodes a functional CDC26 ortholog in plants, forming part of the plant APC/C complex. The CDC26 subunit shows a monocistronic gene architecture in other eukaryotes, but is encoded in a bicistronic transcript upstream of the inorganic polyphosphatase TTM3 in the entire green lineage, from algae to higher land plants (Supplementary Fig. 3). Our genetic analyses suggest no strong functional connection between AtCDC26 (which our analyses define as an essential gene) and AtTTM3 (whose enzymatic function appears to be dispensable, at least in the growth conditions tested, compare Fig. 2), and AtTTM3 does not seem to interact biochemically with stand-alone CDC26 or the plant APC/C (Fig. 3g, Supplementary Fig. 4). It is however of note that inorganic polyphosphates promote cell cycle exit in bacteria[40] and fungi[41], and we thus cannot exclude a functional connection between TTM3 and CDC26.

We did not observe regulation of the *TTM3* mORF by the *CDC26* uORF, but rather we found that translation of the mORF recruited the bicistronic transcript to polysomes, enhancing CDC26 translation and thus CDC26 protein levels *in planta*. While the mechanism of concerted CDC26 and TTM3 translation remains to be investigated, we found that in some species both ORFs are located at a very short distance, or even overlap (Supplementary Fig. 3). This makes *TTM3* translation by ribosome re-initiation unlikely[42]. We confirmed that transcripts featuring an overlapping arrangement of *CDC26* and *TTM3* ORFs are translated in wheat germ extracts, leading to full-length CDC26 and TTM3 protein products

(Supplementary Fig. 7). In addition, we could not detect an internal ribosome entry site (IRES) in the *CDC26* coding sequence, and a synthetic *CDC26-TTM3* transcript with altered codons did still support translation of both proteins (Supplementary Fig. 7). We thus speculate that leaky ribosome scanning may reach the *TTM3* start codon[43], as it has been previously suggested for viral bi-/polycistronic transcripts translated in plants[16,44]. In line with this, the CDC26 start codon from different species is compatible with leaky scanning (ATG**T** or AGT**C**, see Supplementary Fig. 3)[45,46] and we do not observe major changes in CDC26 and TTM3 expression upon treatment with TOR inhibitors, with TOR affecting ribosome re-initiation in plants[7,38]. We could however confirm that the *CDC26-TTM3* transcript is a target of nonsense-mediated decay, which could represent an additional regulatory layer for CDC26 function in cell cycle control (Fig. 6).

Taken together, we demonstrate that the cell cycle regulator AtCDC26 is expressed from a conserved uORF in a gene coding for a metabolic enzyme. Our genetic and biochemical characterization of the *CDC26 TTM3* locus now enables the mechanistic dissection of bicistronic transcription and translation in plants.

METHODS

Plant material and growth conditions. *ttm3-1* (SALK_133625) and *ttm3-4* (SALK_050319) T-DNA insertion lines were obtained from NASC (Nottingham Arabidopsis Stock Center, UK), and *ttm3-2* (FLAG_368E06) from Arabidopsis Stock Center in Versailles (France). The *ttm3-3* mutant was generated using CRISPR/Cas9. Specifically, the *TTM3*-specific sequence 5'-ATTGAGACGGAGATGAGCAGCGG-3' (*sgTTM3*) was cloned into the PTTK352 vector[47], containing Cas9 in a cassette with hygromycin-resistance and RFP as selection-markers. *Arabidopsis* Col-0 plants were transformed with pTTK352-sg*TTM3* (see *generation of transgenic lines*). T1 generation plants were selected via hygromycin resistance. *ttm3-3* was identified by PCR followed by sequencing. In T2 generation, seeds not expressing RFP (lacking Cas9) were selected. Plants were grown at 50 % humidity, 22 °C and 16/8 h light-dark-cycles.

Real-time quantitative reverse transcription polymerase chain reaction. RNA was extracted with the Rneasy Plant Mini Kit (Qiagen). 2 µg of RNA was treated with Dnase I (Qiagen), copied to cDNA using an Oligo dT and the SuperScript™ II Reverse Transcriptase (Invitrogen). Transcript levels were estimate using the SYBR Green PCR Master Mix (Applied Biosystems), and transcript abundance was normalized to *ACT8*. Values indicate the mean ± standard deviation of three technical replicates. Primer sequences can be found in Supplementary Table 2.

Protein expression and generation of antibodies. TTM3 was produced and purified as described[23]. For generation of the TTM3 antibody, rabbits were immunized with purified TTM3 dialyzed against phosphate-buffered saline (PBS). The resulting serum was affinity-

purified over a AtTTM3-coupled Affigel 15 affinity column (Biorad, www.bio-rad.com), eluted in 200 mM glycine pH 2.3, 150 mM NaCl and stored in PBS pH 7.5.

CDC26 was cloned into pMH-TrxT vector, providing an N-terminal 6xHis-StrepII-Thioredoxin tag (HST) and a tobacco etch virus (TEV) protease cleavage site. CDC26 expression was induced in *Escherichia coli* BL21 (DE3) RIL cells with 0.25 mM isopropyl β-D-galactoside (IPTG) at OD_{600} ~0.6, and grown at 16 °C for 16 h. Cells were collected by centrifugation (4,500 x g, 30 min), resuspended in lysis buffer (20 mM Tris pH 8, 500 mM NaCl, 1 mM $MgCl_2$, 5 mM β-mercaptoethanol and cOmplete™ EDTA-free Protease Inhibitor Cocktail [Merck]), and homogenized using an Emulsiflex C-3 (Avestin). HST-CDC26 was isolated from the lysate via tandem Ni^{2+} and StrepII-affinity purification (HisTrap HP 5 ml, GE Healthcare; Strep-Tactin Superflow high capacity, IBA), and purified further by size-exclusion chromatography (Superdex 75 HR10/30, GE Heathcare, equilibrated with 50 mM sodium phosphate pH 7.5, 500 mM NaCl). The HST-CDC26 fusion protein was incubated with TEV protease (1:100 molar ratio) for 16 h at 4 °C. CDC26 was recovered by a second Ni^{2+}-affinity step followed by size exclusion chromatography. The molecular weight of the purified protein was determined to be 7.3 kDa by MALDI-TOF mass spectrometry. A polyclonal CDC26 antibody was generated in rabbit (Eurogentec) and purified as described for AtTTM3. The characterization of the anti-AtCDC26 antibody is presented in Supplementary Fig. 8.

Western blotting. Plant material was snap-frozen in liquid nitrogen and homogenized with mortar and pestle. The material was resuspended in 50 mM Tris pH 8.0, 150 mM NaCl, 0.5 % Triton X-100 and cOmplete™ EDTA-free Protease Inhibitor Cocktail (Merck). 20-50 µg

of total protein extract (estimated by Bradford, Bio-Rad), pre-boiled for 5 min, was run on a 10 % SDS-PAGE gel. Proteins were blotted onto nitrocellulose membranes (GE Healthcare), then blocked using TBS buffer containing 0.1 % (v/v) tween 20, 5 % (w/v) powder milk. Membranes were incubated for 1 h at room temperature with CDC26 or TTM3 antibodies, and then with an anti-rabbit peroxidase conjugate antibody from Calbiochem (dilution 1:10,000), or with an anti-HA-HRP (Miltenyi Biotec) (dilution 1:5,000). Membranes were then stained with Ponceau (0.1 % [w/v] Ponceau S in 5 % [v/v] acetic acid). Bands corresponding to RuBisCO (~56 kDa) are shown as loading control.

Phenotyping assays. For root length measurements, stratified seeds (2-5 d, 4 °C, in darkness) were germinated on ½ MS medium, containing ½ MS (Duchefa), 0.5 g/L MES, 0.8 % (w/v) agar, 1 % (w/v) sucrose, pH 5.7. After 4 d, seedlings were transferred to new plates and grown for 7 d at 22 °C, 16 h of light. For hypocotyl length measurements, seeds were plated in ½ MS and exposed 3 h to light after 2-5 d of stratification (4 °C, in darkness). Seedlings were grown for 6 d in darkness at 22 °C. Measurements were done using the NeuronJ plugin[48] in Fiji[49]. The simultaneous comparisons of root and hypocotyl growth against wild type for a fold change was performed for a Dunnett-type procedure ratio-to-control[50] assuming approximate normal distributed variance heterogeneous errors using the package ’mratios’ in R-CRAN. Adjusted two-sided p-values are reported in figure legends.

For germination assays, seeds were plated in ½ MS and stratified for 2-5 d at 4 °C in darkness. Germination rates were determined after 2 d of light exposure. Imaging of *ttm3-2* embryos was performed by opening siliques from *ttm3-2* heterozygous plants. Seeds were mounted on a cover slip and covered by a destaining solution containing 2.7 g/l chloral

hydrate, 0.25 % (v/v) glycerol. Samples were destained for 16 h at 4 °C and imaged under a conventional light microscope.

Generation of transgenic lines. For constructs cloned in pH7m34GW (pH7) and pB7m34GW (pB7)[51] vectors (compare Supplementary Table 1), promoters were cloned first into the pDONR P4-P1R vector, coding sequences into pDONR221 or pDONR207 vectors, and C-terminal tags into pDONR P2R-P3 vector with the Gateway™ BP Clonase™ II Enzyme mix (Merck). Constructs were assembled by the Gateway™ LR Clonase™ Enzyme mix (Merck). Some constructs were cloned into the pGreenII vector (pGIIB) (GenBank reference: EF590266.1) or in a modified-version, pGIIH, by Gibson assembly[52], to avoid the overhands created by gateway cloning. In the pGIIH vector, the gene conferring resistance to Basta was replaced by a hygromycine resistance gene cassette by Gibson cloning[52]. *Agrobacterium tumefaciens*, strain pGV2260, was transformed with pH7, pB7, or with the binary vectors pGIIH or pGIIB (pSOUP was used as a help plasmid, GenBank reference: EU048870.1). *Arabidopsis thaliana* was transformed using the floral dip method[53]. T1 plants were selected using hygromycin (pH7, pGIIH) or Basta (pB7, pGIIB), and homozygous plants were analyzed in T3 generation.

β-glucuronidase (GUS) reporter assay. Plants or plant organs were fixed in 2 % (v/v) formaldehyde, 50 mM sodium phosphate buffer pH 7.0 for 30 min at room temperature. After two washes with 50 mM sodium phosphate buffer, plants were submerged into a staining solution containing 0.5 mM potassium ferrocyanide, 0.5 mM potassium ferricyanide and 0.1 mM X-GlcA. Vacuum was applied 3 times, 1 min per pulse. Staining occurred for 2 h at 37 °C. After washing samples twice (1 h incubation per wash) with 96 % (v/v) ethanol and 60 % (v/v) ethanol, respectively, plants were stored in 20 % (v/v) ethanol. Pictures were taken with

a Canon EOS 1000D SLR digital camera coupled to a stereomicroscope Zeiss SteREO DiscoveryV8.

Isothermal titration calorimetry (ITC). CDC26 and TTM3 interaction was assayed using a Nano ITC (TA Instruments) at 25 °C. Both proteins were gel-filtrated into ITC buffer (20 mM Tris pH 8, 500 mM NaCl, 1 mM $MgCl_2$). 200 µM CDC26 was injected into 50 µM TTM3 protein, in 25 injections at 150 s intervals (10 µL per injection). Data was corrected for the dilution heat and analyzed using the software NanoAnalyze (version 3.5) provided by the manufacturer.

Immunoprecipitation followed by LC-MS. Ws-4 wild-type and pUBI10:CDC26-6xHA seedlings were snap-frozen in liquid nitrogen, homogenized with mortar and pestle and resuspended in protein extraction buffer (PBS buffer pH 7.4, 1 mM EDTA, cOmplete™ EDTA-free Protease Inhibitor Cocktail from Merck) including 0.1 % (v/v) Triton X-100. The lysate was incubated with anti-HA microbeads (µMACS HA Isolation Kit, Miltenyi Biotec) at 4 °C for 2 h. Beads were washed 4 times with protein extraction buffer supplemented with 0.05 % (v/v) Triton X-100, 1 time with protein extraction buffer, and eluted with the denaturing elution buffer provided in the kit. The elution was boiled for 5 min at 95 °C and separated into a 10 % SDS-PAGE gel. Silver staining was performed as previously described[54]. Bands present in the pUBI10:CDC26-6xHA sample and absent or reduced in the Ws-4 sample were cut and analyzed by LC-MS at the Proteomics Core Facility (Centre Medical Universitaire, CMU, Geneva). Results were analyzed using the software Scaffold (Proteome Software Inc, Portland, Oregon), setting a threshold of 99.9 % for peptide and protein identification.

RNA extraction and northern blot. Col-0 wild-type and *ttm3-1* mutant seedlings were snap-frozen in liquid nitrogen and homogenized with mortar and pestle. RNA was isolated using TRIZOL (Gibco BRL, Grand Island, NY, USA) according to the supplier's instructions. 5 µg of total RNA was treated with DnaseI (Qiagen) and recovered with the standard phenol-chloroform purification[55] (UltraPure™ Phenol:Chloroform:Isoamyl Alcohol [25:24:1, v/v], Merk). Samples containing 7 µg of RNA, 0.1 % (v/v) formaldehyde and 1x MOPS buffer (20 mM MOPS pH 7.0, 5 mM NaOAc, 1 mM EDTA) were heated for 15 min at 60 °C, and loaded into a formaldehyde gel with 1 % (w/v) agarose, 1x MOPS, 1 % (v/v) formaldehyde. Electrophoresis was performed for 3 h at 60 V in MOPS buffer. The gel was blotted overnight in a hybond-N membrane (GE Healthcare) in 10x SSC buffer (150 mM sodium citrate, 1.5 M NaCl). The membrane was UV cross-linked and pre-hybridized with church buffer (0.25 M PBS pH 7.2, 1 mM EDTA. 1 % [w/v] BSA and 7 % [w/v] SDS) for 45 min at 65 °C. 50 ng of the respective *CDC26* and *TTM3* probes (Supplementary Table 2), labeled with dCTP[α-^{32}P] (PerkinElmer), were hybridized overnight at 65 °C. Membranes were washed with 1x SSC buffer supplemented with 0.1 % SDS, and subsequently exposed to an X-ray film for 3 d at -80 °C.

5’ and 3’ Rapid amplification of cDNA ends (RACE). 3’ RACE was performed using the Thermofisher 3’ RACE kit following the manufacturer’s instructions. For the 5’RACE, RNA was copied to cDNA using RACE_SP1 primer (compare Supplementary Table 2). A polyA tail was added artificially with a terminal transferase (NEB) using ATP as substrate. The cDNA was used as a template in a second PCR with an oligo dT fused to an adaptor primer (AP) and RACE_SP2 primer. A third PCR with RACE_SP3 and AUAP gave a 5’ RACE specific product. The major band was cut and sent for sequencing with TTM3_3’_F and

CDC26_RT_F primers (compare Supplementary Table 2). Alternatively, RACE products were cloned in pCR™8 (Merck) and sequenced with M13 forward and T7 forward primers.

***In vitro* transcription and translation.** *CDC26-TTM3* transcript (including the *CDC26* start codon and 1268 down-stream base-pairs) was cloned into pCR™8 (Merck), under the control of the T7 promoter. Mutations were performed by site-directed mutagenesis (see Supplementary Table 2). Capped RNA was transcribed *in vitro* using the MEGAscript™ T7 Transcription Kit (Merck). 1 µg of RNA was added to wheat germ extract (Promega), and *in vitro* translation was performed as recommended by the manufacturer. Products from the *in vitro* translation, labeled with ^{35}S methionine, were loaded onto a 12 % polyacrylamide gel and run for ~ 2 h at 100 V. The gel was washed with water and exposed to a X-ray film for 4 h at -80 °C.

Confocal microscopy. CYCB1;1-GFP seeds were crossed with the *ttm3-1* mutant allele. Selection of CYCB1;1 insertion was done via Basta selection, and the presence of the *ttm3-1* insertion was confirmed by genotyping. Plants were analyzed in F3 generation. 4 d old seedlings were fixed in PBS with 4 % (v/v) paraformaldehyde and 0.01 % (v/v) Triton X-100 for 1 h at room temperature after vacuum infiltration. Samples were washed twice in PBS and incubated for one week in the dark at room temperature in ClearSee solution[56]. Next, samples were mounted between slide and coverslip in ClearSee solution and imaged under an SP8 confocal microscope (Leica) equipped with a 10x NA 0.3 lens and a HyD detector using 488 nm excitation and 492-533 nm emission, a pinhole of 1AU and a pixel size of 180 nm. Number of GFP-expressing cells was quantified[57] using the software Fiji[49]. The transmission image was used to estimate cell length; the last cortical cell, the length of which was

approximately 1.5 times its width, was defined as the last cortical meristematic cell and was used to define the limit of the meristem. Maximal intensity projections of the confocal z stacks were performed and the look-up table “Fire” was used to optimize the visualization of GFP signal. Localization of the TTM3-mCITRINE fusion protein was analyzed in 5 d old seedlings again using the SP8 confocal microscope.

Polysome profiling. Wild-type and two independent transgenic lines expressing CDC26-*TTM3 (in *ttm3-2* background) were grown for 10 d in ½ MS medium. Alternatively, 7 d old wild-type seedlings were treated for 4 h in 1/8 MS liquid medium containing either 1 µM AZD or DMSO (mock). Seedlings were snap-frozen and homogenized with mortar and pestle. The material was resuspended in 1 volume of polysome extraction buffer, containing 200 mM Tris pH 9.0, 200 mM KCl, 1 % deoxycholate, 1 % polyoxyethylene 10 tridecyl ether, 35 mM $MgCl_2$, 1 mM DTT and 100 µg/mL cycloheximide. After 15 min incubation on ice, the cell extract was centrifuged for 15 min at 16,000 x g, 4 °C. The clarified extract was loaded on top of a 15 % to 60 % sucrose gradient. Polysomal fractions were separated by ultracentrifugation on a SW55 rotor (Beckman), at 290,000 x g 1 h 15 min, 4 °C, and collected from top to bottom into 10 fractions using a gradient holder (Brandel) coupled to a spectrophotometer. RNA from each fraction was extracted using TRIZOL (Gibco BRL, Grand Island, NY, USA), according to the supplier's instructions. After a second RNA precipitation (500 mM ammonium acetate, 2.5 volumes of ethanol, 1 h, -20 °C), RNA was reverse transcribed into cDNA using the M-MLV RNAse H minus kit (Promega) and oligo dT, and analyzed by qRT-PCR as described above. The fraction 1 was excluded from the analysis since it contained very low amount of both *TTM3* and *ACT* mRNAs. The percentage of TTM3 mRNA in each fraction (relative to *ACT2*) was determined as described[58].

Data availability. Authors confirm that all relevant data has been included in this paper and it is available upon reasonable request. *Arabidopsis* mutant accessions *ttm3-1* (SALK_133625) and *ttm3-4* (SALK_050319) are available at the Nottingham Arabidopsis Stock Center (NASC, http://arabidopsis.info/). *ttm3-2* (FLAG_368E06, EMBL number AJ838411) is available at the Versailles Arabidopsis Stock Center (http://publiclines.versailles.inra.fr/).

FIGURE LEGENDS

Figure 1 | Different *ttm3* mutant alleles show inconsistent phenotypes related to embryo development and plant growth. a, Overview of *ttm3* alleles in the *TTM3* locus. **b**, *TTM3* transcript in *ttm3* mutants relative to wild-type, estimated by qPCR (left) with TTM3_RT_F/R primers (see Supplementary Table 2). cDNA was obtained from ~100 seedlings per genotype. Columns define mean values, error bars represent standard deviation (SD) of n=3 technical replicates. TTM3 protein levels were determined by western blot (right) (experiment performed twice with similar results). **c**, Developing wild-type and *ttm3-2* embryos in different stages (scale bars are 20 µm). Quantification of embryo-developmental phenotypes in seeds from *ttm3-2* heterozygous plants is shown alongside. **d**, Root growth assay with *ttm3* mutants and wild-type. Representative seedlings are shown on the left. Root length measurements of wild-type and *ttm3* mutant seedlings (normalized to wild-type) are represented with box plots (right) (n=13 seedlings per genotype). Box plots span the first to third quartiles, whiskers indicate minimum and maximum values. Two-sided adjusted p-values are reported for simultaneous comparisons from a Dunnett-type procedure ratio-to-control[50] (*ttm3-1*/wild-type < 0.001, *ttm3-3*/WT = 0.693, *ttm3-4*/WT = 0.019). **e**, Hypocotyl growth assay (n=62 seedlings per genotype). Representative seedlings are shown on the left.

Hypocotyl length measurements (normalized to wild-type) are represented with dots on the right, lines indicate median values. Two-sided adjusted p-values are reported for simultaneous comparisons from a Dunnett-type procedure ratio-to-control[50] (*ttm3-1*/WT < 0.001, *ttm3-3*/WT < 0.001, *ttm3-4*/WT = 0.002).

Figure 2 | Catalytically inactive TTM3 variants complement *ttm3* phenotypes when expressed from the native promoter including the 5' UTR. a, Complementation of the embryo lethal *ttm3-2* allele with pTTM3:TTM3-mCITRINE restores seed germination, as seen in two independent transgenic lines (#41 and #44). Shown are representative seedlings with the corresponding germination rates (%) and total number of seeds in brackets. Scale bars correspond to 0.5 cm. **b**, Root growth assay with *ttm3-1* plants expressing pTTM3:TTM3-mCITRINE. Representative seedlings are shown on the left. Root length measurements of wild-type, *ttm3-1* and 2 independent transgenic lines (#8 and #12) (normalized to wild-type) are represented in box plots (right) (n=12 seedlings per genotype). Box plots span the first to third quartiles, whiskers indicate minimum and maximum values. Two-sided adjusted p-values are reported for simultaneous comparisons using a Dunnett-type procedure ratio-to-control[50] (#8/WT = 0.479, #12/WT = 0.600). **c,** Ribbon diagram of the AtTTM3 tunnel domain (PDB-ID: 5A67[23], in yellow) with a triphosphate molecule bound in the center, coordinated by a Mn^{2+} ion (pink sphere). Arg52 (involved in substrate binding[23]) is shown in cyan, three glutamate residues required for metal co-factor binding and catalysis[23] are highlighted in magenta (Glu2, Glu4 and Glu169). **d**, AtTTM3 mutant proteins, impaired in either substrate binding or catalysis fully complement the *ttm3-2* mutant phenotype when expressed from the *TTM3* promoter including the annotated 5' UTR, as judged from seed germination assays. Shown are germination rates (%), with total number of seeds in brackets.

e, TTM3-mCITRINE is expressed at lower levels than endogenous TTM3, as judged from western blotting (experiment repeated more than 3 times, with similar outcome). **f,** CDC26, translated from the *TTM3* 5'UTR, is expressed at wild-type levels in seedlings producing TTM3-mCITRINE fusions (experiment repeated more than 3 times with similar results).

Figure 3 | A uORF in *TTM3* encodes the cell-cycle regulator AtCDC26. a, Arabidopsis *CDC26* maps to the 5' UTR of *TTM3* and contains the N-terminal CDC26 motif required for APC/C binding conserved among different CDC26 orthologs. **b**, CDC26 and TTM3 proteins are expressed in different tissues and stages of development, as judged by western blot (experiment repeated twice with similar results). **c**, *CDC26* transcript levels in *ttm3* mutants relative to wild-type, measured by qPCR (left) using CDC26_RT_F/R primers (see Supplementary Table 2). cDNA was obtained from ~100 seedlings per genotype. Columns define mean values, error bars represent SD of n=3 technical replicates. CDC26 protein levels were determined by western blot (right; experiment performed twice with similar results). **d**, Complementation of *ttm3-2* with pUBI10:CDC26-6xHA restores seed germination, as seen in 2 independent transgenic lines (#1 and #9). Shown on the left are percentages of germinated seeds, total number of seeds in brackets (scale bars=0.5 cm). AtCDC26-6xHA protein levels were detected by western blot using an anti-HA antibody (right, experiment repeated more than 3 times, with similar results). **e**, Root growth assay with *ttm3-1* plants complemented with pUBI10:CDC26-6xHA. Root length measurements of wild-type, *ttm3-1* and 2 independent transgenic lines (#6 and #8), normalized to wild-type average, are represented in box plots (n=24 seedlings per genotype). Box plots (right) span the first to third quartiles, whiskers indicate minimum and maximum values. Two-sided adjusted p-values are reported for simultaneous comparisons using a Dunnett-type procedure ratio-to-control[50]

(#8/WT=0.920, #6/WT=0.017). **f,** Hypocotyl growth assays in *ttm3-1* complemented with pUBI10:CDC26-6xHA (n=53 seedlings per genotype). Dots represent hypocotyl length measurements normalized to wild-type average, lines indicate median values (left). Two-sided adjusted p-values are reported for simultaneous comparisons using a Dunnett-type procedure ratio-to-control[50] (#6/WT=0.037, #8/WT=0.447). Western blot (right) shows expression of CDC26-6xHA (experiment performed more than 3 times, with similar results). **g**, APC/C components recovered by IP-MS (arrows indicate bands present in CDC26-6xHA and absent or reduced in wild-type). The experiment was performed twice with a similar outcome. AtCDC26 protein interactors are highlighted in the human APC/C structure (PDB-ID 4ui9[27]) (bottom). **h**, Root tips of *ttm3-1* plants expressing pCYCB1;1:CYCB1;1-GFP show less GFP expressing-cells and an overall lower GFP intensity compared to wild-type plants expressing CYCB1;1-GFP (scale bars correspond to 25 μm). Box plots (right) span the first to third quartiles, whiskers indicate minimum and maximum values (n=6 seedlings per genotype).

Figure 4 | CDC26 is expressed from a bicistronic transcript in plants. a, Phylogenetic tree of *CDC26* and *TTM3* ORFs from different plant species. Distances between the *CDC26* termination codon and the *TTM3* start codon are indicated in base-pairs, branch lengths are arbitrary. **b**, Northern blots using two different probes (scheme shown below) reveals a major transcript detected with *CDC26* and *TTM3* probes and absent in *ttm3-1* plants (indicated with an arrow). Experiment were repeated 3 times with similar results. **c**, RACE experiments result in cDNA products containing either *CDC26* and *TTM3* ORFs or *CDC26* alone (marked by arrows), as shown in a scheme containing transcript length (see sequences in Supplementary Information). *ttm3-1* harbors a truncated transcript containing only the

CDC26 uORF. RACE experiments were performed 3 times with similar results. **d**, RT-PCR using primers binding to *CDC26* and *TTM3* confirm the presence of a single *CDC26-TTM3* transcript (blue), absent in *ttm3-1*, and a CDC26 transcript (red), present in low levels in *ttm3-1*. A scheme is shown alongside, indicating the expected products (see Supplementary Table 2 for primer sequences). Two independent experiments showed similar results. **e**, *In vitro* translation of an *in vitro* transcribed *CDC26-TTM3* bicistronic transcript results in two proteins of the expected molecular weight (7.225 kDa for AtCDC26 and 24.162 kDa for AtTTM3, compare Supplementary Fig. 8). Mutation of the *CDC26* or *TTM3* start codon blocks translation of the respective protein. Similar results were observed in 3 independent experiments.

Figure 5 | TTM3 translation recruits the bicistronic transcript to polysomes. a, Transcripts containing mutations in *CDC26* and *TTM3* start codons (*CDC26 and *TTM3, respectively) used for complementation of *ttm3-2* plants. Expression was done using the endogenous promoter. **b**, *CDC26 does not complement *ttm3-2* embryo-lethality in 4 independent transgenic lines. **c**, *TTM3 phenotypes are reminiscent of *apc* loss-of-function mutants (top). Details of wild-type and *TTM3 siliques (bottom, scale bar is 2 cm). Similar phenotypes were observed in 3 independent plant growth assays. **d**, CDC26 protein levels are reduced in *TTM3 plants (top, experiment repeated twice with similar outcome), while transcript levels are higher than wild-type (bottom, primer sequences TTM3_RT_F/R in Supplementary Table 2). cDNA was obtained from leaves of individual plants, experiments were performed twice with similar outcome. Columns indicate mean values, error bars denote SD for n=3 technical replicates. **e**, Polysome profile (top) reveals that the bicistronic transcript associates with polysomes in wild-type but not in *TTM3 (bottom) plants (primers

TTM3_RT_F/R, see Supplementary Table 2). Y values indicate the mean, error bars denote SD for n=3 technical replicates. Polysome profiling was performed 2 times with similar results.

Figure 6 | The CDC26-TTM3 transcript is a target of NMD. a, Treatment of 5 d old wild-type plants with 20 µM cycloheximide (CHX) for 8 h leads to the accumulation of *SMG7* (a known NMD target) and *CDC26-TTM3* transcripts, as concluded from qPCR experiments (see Supplementary Table 2 for primer sequences). cDNA was obtained from ~30 seedlings per genotype. Columns indicate mean values, error bars denote SD for n=3 technical replicates. **b,** *CDC26-TTM3* transcript levels are slightly higher in Arabidopsis *lba1* and *upf3-1* mutants as seen in qPCR experiments (see Supplementary Table 2 for primer sequences). cDNA was obtained from ~100 seedlings per genotype. Columns indicate mean values, error bars denote SD for n=3 technical replicates. **c**, CDC26 and TTM3 protein levels are higher in NMD mutants when compared to the actin control (experiment performed 2 times with similar results).

References

1. Oyama, M. *et al.* Analysis of small human proteins reveals the translation of upstream open reading frames of mRNAs. *Genome Res.* **14**, 2048–2052 (2004).
2. Johnstone, T. G., Bazzini, A. A. & Giraldez, A. J. Upstream ORFs are prevalent translational repressors in vertebrates. *EMBO J.* **35**, 706–723 (2016).
3. Wethmar, K. The regulatory potential of upstream open reading frames in eukaryotic gene expression. *RNA* **5**, 765–778 (2014).

4. Wethmar, K., Barbosa-Silva, A., Andrade-Navarro, M. A. & Leutz, A. uORFdb--a comprehensive literature database on eukaryotic uORF biology. *Nucleic Acids Res.* **42**, D60-67 (2014).
5. Menschaert, G. *et al.* Deep proteome coverage based on ribosome profiling aids mass spectrometry-based protein and peptide discovery and provides evidence of alternative translation products and near-cognate translation initiation events. *Mol. Cell. Proteomics* **12**, 1780–1790 (2013).
6. von Arnim, A. G., Jia, Q. & Vaughn, J. N. Regulation of plant translation by upstream open reading frames. *Plant Sci.* **214**, 1–12 (2014).
7. Schepetilnikov, M. *et al.* TOR and S6K1 promote translation reinitiation of uORF-containing mRNAs via phosphorylation of eIF3h. *EMBO J.* **32**, 1087–1102 (2013).
8. Zhou, F., Roy, B., Dunlap, J. R., Enganti, R. & von Arnim, A. G. Translational control of Arabidopsis meristem stability and organogenesis by the eukaryotic translation factor eIF3h. *PLoS ONE* **9**, (2014).
9. Pajerowska-Mukhtar, K. M. *et al.* The HSF-like transcription factor TBF1 is a major molecular switch for plant growth-to-defense transition. *Curr. Biol.* **22**, 103–112 (2012).
10. Starck, S. R. *et al.* Translation from the 5' untranslated region shapes the integrated stress response. *Science* **351**, aad3867 (2016).
11. Wiese, A., Elzinga, N., Wobbes, B. & Smeekens, S. A Conserved Upstream Open Reading Frame Mediates Sucrose-Induced Repression of Translation. *Plant Cell* **16**, 1717–1729 (2004).
12. Kurihara, Y. *et al.* Genome-wide suppression of aberrant mRNA-like noncoding RNAs by NMD in Arabidopsis. *Proc. Natl. Acad. Sci. U. S. A.* **106**, 2453–2458 (2009).
13. Nyikó, T., Sonkoly, B., Mérai, Z., Benkovics, A. H. & Silhavy, D. Plant upstream ORFs can trigger nonsense-mediated mRNA decay in a size-dependent manner. *Plant Mol. Biol.* **71**, 367–378 (2009).

14. Malabat, C., Feuerbach, F., Ma, L., Saveanu, C. & Jacquier, A. Quality control of transcription start site selection by nonsense-mediated-mRNA decay. *eLife* **4**, doi: 10.7554/eLife.06722 (2015).

15. Mouilleron, H., Delcourt, V. & Roucou, X. Death of a dogma: eukaryotic mRNAs can code for more than one protein. *Nucleic Acids Res.* **44**, 14–23 (2016).

16. Ryabova, L. A., Pooggin, M. M. & Hohn, T. Translation reinitiation and leaky scanning in plant viruses. *Virus Res.* **119**, 52–62 (2006).

17. Lee, S. J. Expression of growth/differentiation factor 1 in the nervous system: conservation of a bicistronic structure. *Proc. Natl. Acad. Sci. U. S. A.* **88**, 4250–4254 (1991).

18. Ouelle, D. E., Zindy, F., Ashmun, R. A. & Sherr, C. J. Alternative reading frames of the INK4a tumor suppressor gene encode two unrelated proteins capable of inducing cell cycle arrest. *Cell* **83**, 993–1000 (1995).

19. Klemke, M., Kehlenbach, R. H. & Huttner, W. B. Two overlapping reading frames in a single exon encode interacting proteins—a novel way of gene usage. *EMBO J.* **20**, 3849–3860 (2001).

20. Lee, C., Lai, H.-L., Lee, Y.-C., Chien, C.-L. & Chern, Y. The A2A adenosine receptor is a dual coding gene. *J. Biol. Chem.* **289**, 1257–1270 (2014).

21. Autio, K. J. *et al.* An ancient genetic link between vertebrate mitochondrial fatty acid synthesis and RNA processing. *FASEB J.* **22**, 569–578 (2008).

22. Moeder, W. *et al.* Crystal structure and biochemical analyses reveal that the Arabidopsis triphosphate tunnel metalloenzyme AtTTM3 is a tripolyphosphatase involved in root development. *Plant J.* **76**, 615–626 (2013).

23. Martinez, J., Truffault, V. & Hothorn, M. Structural determinants for substrate binding and catalysis in triphosphate tunnel metalloenzymes. *J. Biol. Chem.* **290**, 23348–23360 (2015).

24. Vaughn, J. N., Ellingson, S. R., Mignone, F. & Arnim, A. von. Known and novel post-transcriptional regulatory sequences are conserved across plant families. *RNA* **18**, 368–384 (2012).

25. Capron, A., Okrész, L. & Genschik, P. First glance at the plant APC/C, a highly conserved ubiquitin-protein ligase. *Trends Plant Sci.* **8**, 83–89 (2003).

26. Lima, M. de F. *et al.* Genomic evolution and complexity of the Anaphase-promoting Complex (APC) in land plants. *BMC Plant Biol.* **10**, 254 (2010).

27. Chang, L., Zhang, Z., Yang, J., McLaughlin, S. H. & Barford, D. Atomic structure of the APC/C and its mechanism of protein ubiquitination. *Nature* **522**, 450–454 (2015).

28. Hutchins, J. R. A. *et al.* Systematic analysis of human protein complexes identifies chromosome segregation proteins. *Science* **328**, 593–599 (2010).

29. Zachariae, W., Shin, T. H., Galova, M., Obermaier, B. & Nasmyth, K. Identification of subunits of the anaphase-promoting complex of Saccharomyces cerevisiae. *Science* **274**, 1201–1204 (1996).

30. Genschik, P., Marrocco, K., Bach, L., Noir, S. & Criqui, M.-C. Selective protein degradation: a rheostat to modulate cell-cycle phase transitions. *J. Exp. Bot.* **65**, 2603–2615 (2014).

31. Ubeda-Tomás, S. *et al.* Gibberellin signaling in the endodermis controls Arabidopsis root meristem size. *Curr. Biol.* **19**, 1194–1199 (2009).

32. Genschik, P., Criqui, M. C., Parmentier, Y., Derevier, A. & Fleck, J. Cell cycle - dependent proteolysis in plants. Identification of the destruction box pathway and metaphase arrest produced by the proteasome inhibitor MG132. *Plant Cell* **10**, 2063–2076 (1998).

33. Criqui, M. C. *et al.* Cell cycle-dependent proteolysis and ectopic overexpression of cyclin B1 in tobacco BY2 cells. *Plant J.* **24**, 763–773 (2000).

34. Dickinson, M. E. *et al.* High-throughput discovery of novel developmental phenotypes. *Nature* **537**, 508–514 (2016).

35. Cornelis, S. *et al.* Identification and characterization of a novel cell cycle-regulated internal ribosome entry site. *Mol. Cell* **5**, 597–605 (2000).

36. Marrocco, K., Thomann, A., Parmentier, Y., Genschik, P. & Criqui, M. C. The APC/C E3 ligase remains active in most post-mitotic Arabidopsis cells and is required for proper vasculature development and organization. *Development* **136**, 1475–85 (2009).

37. Zheng, B., Chen, X. & McCormick, S. The Anaphase-promoting complex is a dual integrator that regulates both microRNA-mediated transcriptional regulation of cyclin B1 and degradation of cyclin B1 during Arabidopsis male gametophyte development. *Plant Cell* **23**, 1033–1046 (2011).

38. Schepetilnikov, M. & Ryabova, L. A. Recent discoveries on the role of TOR (Target of Rapamycin) signaling in translation in plants. *Plant Physiol.* **176**, 1095–1105 (2018).

39. Rayson, S. *et al.* A role for nonsense-mediated mRNA decay in plants: pathogen responses are induced in Arabidopsis thaliana NMD mutants. *PloS One* **7**, e31917 (2012).

40. Racki, L. R. *et al.* Polyphosphate granule biogenesis is temporally and functionally tied to cell cycle exit during starvation in Pseudomonas aeruginosa. *Proc. Natl. Acad. Sci. U. S. A.* **114**, E2440–E2449 (2017).

41. Bru, S. *et al.* Polyphosphate is involved in cell cycle progression and genomic stability in Saccharomyces cerevisiae. *Mol. Microbiol.* **101**, 367–380 (2016).

42. Kozak, M. Constraints on reinitiation of translation in mammals. *Nucleic Acids Res.* **29**, 5226–5232 (2001).

43. Kozak, M. Pushing the limits of the scanning mechanism for initiation of translation. *Gene* **299**, 1–34 (2002).

44. Matsuda, D. & Dreher, T. W. Close spacing of AUG initiation codons confers dicistronic character on a eukaryotic mRNA. *RNA* **12**, 1338–1349 (2006).

45. Kozak, M. Recognition of AUG and alternative initiator codons is augmented by G in position +4 but is not generally affected by the nucleotides in positions +5 and +6. *EMBO J.* **16**, 2482–2492 (1997).

46. Nakagawa, S., Niimura, Y., Gojobori, T., Tanaka, H. & Miura, K. Diversity of preferred nucleotide sequences around the translation initiation codon in eukaryote genomes. *Nucleic Acids Res.* **36**, 861–871 (2008).

47. Tsutsui, H. & Higashiyama, T. pKAMA-ITACHI Vectors for Highly Efficient CRISPR/Cas9-Mediated Gene Knockout in Arabidopsis thaliana. *Plant Cell Physiol.* **58**, 46–56 (2017).

48. Meijering, E. *et al.* Design and validation of a tool for neurite tracing and analysis in fluorescence microscopy images. *Cytom. Part J. Int. Soc. Anal. Cytol.* **58**, 167–176 (2004).

49. Schindelin, J. *et al.* Fiji: an open-source platform for biological-image analysis. *Nat. Methods* **9**, 676–682 (2012).

50. Dilba, G., Bretz, F., Guiard, V. & Hothorn, L. A. Simultaneous confidence intervals for ratios with applications to the comparison of several treatments with a control. *Methods Inf. Med.* **43**, 465–469 (2004).

51. Karimi, M., De Meyer, B. & Hilson, P. Modular cloning in plant cells. *Trends Plant Sci.* **10**, 103–105 (2005).

52. Gibson, D. G. *et al.* Enzymatic assembly of DNA molecules up to several hundred kilobases. *Nat. Methods* **6**, 343–345 (2009).

53. Clough, S. J. & Bent, A. F. Floral dip: a simplified method for Agrobacterium-mediated transformation of Arabidopsis thaliana. *Plant J.* **16**, 735–743 (1998).

54. Chevallet, M., Luche, S. & Rabilloud, T. Silver staining of proteins in polyacrylamide gels. *Nat. Protoc.* **1**, 1852–1858 (2006).

55. Chomczynski, P. & Sacchi, N. Single-step method of RNA isolation by acid guanidinium thiocyanate-phenol-chloroform extraction. *Anal. Biochem.* **162**, 156–159 (1987).

56. Kurihara, D., Mizuta, Y., Sato, Y. & Higashiyama, T. ClearSee: a rapid optical clearing reagent for whole-plant fluorescence imaging. *Development* **142**, 4168–4179 (2015).

57. Hacham, Y. *et al.* Brassinosteroid perception in the epidermis controls root meristem size. *Development* **138**, 839–848 (2011).

58. Faye, M. D., Graber, T. E. & Holcik, M. Assessment of selective mRNA translation in mammalian cells by polysome profiling. *J. Vis. Exp.* e52295 (2014). doi:10.3791/52295

Supplementary Information is available in the online version of the paper (Supplementary Figures 1-8, Supplementary Tables 1 and 2, and Supplementary Information).

Acknowledgments We thank J. M. Perez-Perez for sending us the CYCB1;1-GFP line, A. Wachter for *lba1* and *upf3-1* seeds, and R. Ulm, A. Wachter and N. Geldner for critical reading of the manuscript. This project was supported by an ERC starting grant from the European Research Council under the European Union's Seventh Framework Programme (FP/2007-2013) / ERC Grant Agreement n. 310856, the Max Planck Society, the European Molecular Biology Organisation (EMBO) Young Investigator Programme (to M.H.), the Howard Hughes Medical Institute (International Research Scholar Award; to M.H.) and the Swiss National Fund Sinergia grant (CRSII3-154471; to YP).

Author Contributions L. L-O. and M. H. designed the study, L. L-O. performed the majority of the experiments and analyzed data. J. W. and A. P. characterized *ttm3* insertion lines, the *ttm3-2* embryo phenotype, performed localization experiments and produced the

TTM3 antibody. J. D. and L. L-O designed and performed the polysome profile assays under the supervision of Y.P.. J. M. together with L. L-O. purified the AtCDC26 protein and antibody. S. L. quantified CYCB1;1 levels, Y. J. generated transgenic reporter lines, L. A. H. performed statistical analyses, L. L-O., J. W., S. L., L. A. H. and M. H. analyzed data, and M. H. supervised the study. L. L-O. and M. H. drafted the manuscript and all authors discussed the results, edited and approved the final versions of the manuscript.

Author Information The authors declare no competing financial interests. Correspondence and requests for materials should be addressed to L.L.O. (laura.lorenzo@unige.ch) or M.H. (michael.hothorn@unige.ch).

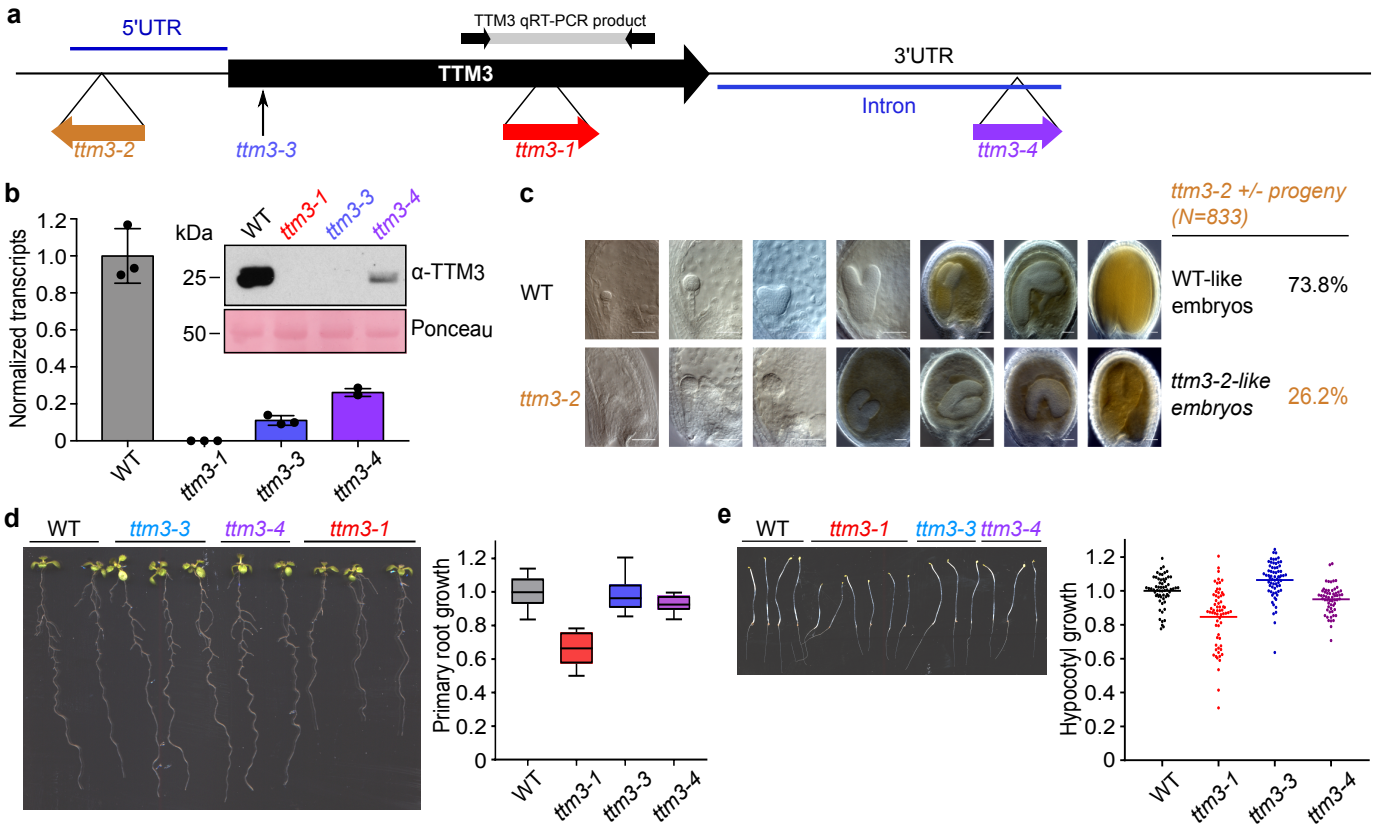
a
5'UTR
TTM3 qRT-PCR product
TTM3
3'UTR
Intron
ttm3-2
ttm3-3
ttm3-1
ttm3-4
b
Normalized transcripts
kDa
WT
ttm3-1
ttm3-3
ttm3-4
25
50
α-TTM3
Ponceau
c
ttm3-2 +/- progeny
(N=833)
WT
ttm3-2
WT-like
embryos
73.8%
ttm3-2-like
embryos
26.2%
d
WT
ttm3-3
ttm3-4
ttm3-1
Primary root growth
e
WT
ttm3-1
ttm3-3
ttm3-4
Hypocotyl growth

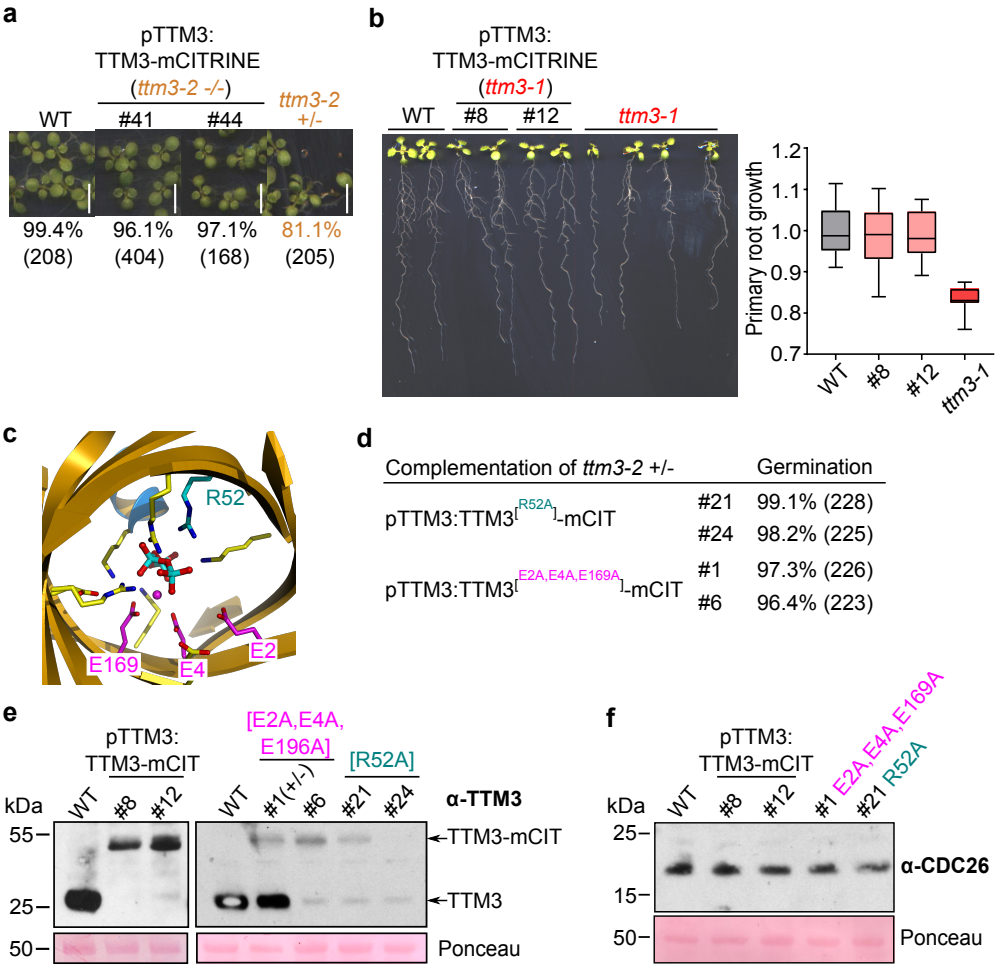
a
pTTM3:
TTM3-mCITRINE
(ttm3-2 -/-)
WT
#41
#44
ttm3-2
+/-
99.4%
(208)
96.1%
(404)
97.1%
(168)
81.1%
(205)
b
pTTM3:
TTM3-mCITRINE
(ttm3-1)
WT
#8
#12
ttm3-1
Primary root growth
1.2
1.1
1.0
0.9
0.8
0.7
WT
#8
#12
ttm3-1
c
R52
E169
E4
E2
d
Complementation of ttm3-2 +/-
Germination
pTTM3:TTM3[R52A]-mCIT
#21
99.1% (228)
#24
98.2% (225)
pTTM3:TTM3[E2A,E4A,E169A]-mCIT
#1
97.3% (226)
#6
96.4% (223)
e
pTTM3:
TTM3-mCIT
[E2A,E4A,
E196A]
[R52A]
kDa
WT
#8
#12
WT
#1(+/-)
#6
#21
#24
α-TTM3
55
25
50
TTM3-mCIT
TTM3
Ponceau
f
pTTM3:
TTM3-mCIT
kDa
WT
#8
#12
#1 E2A,E4A,E169A
#21 R52A
25
15
50
α-CDC26
Ponceau

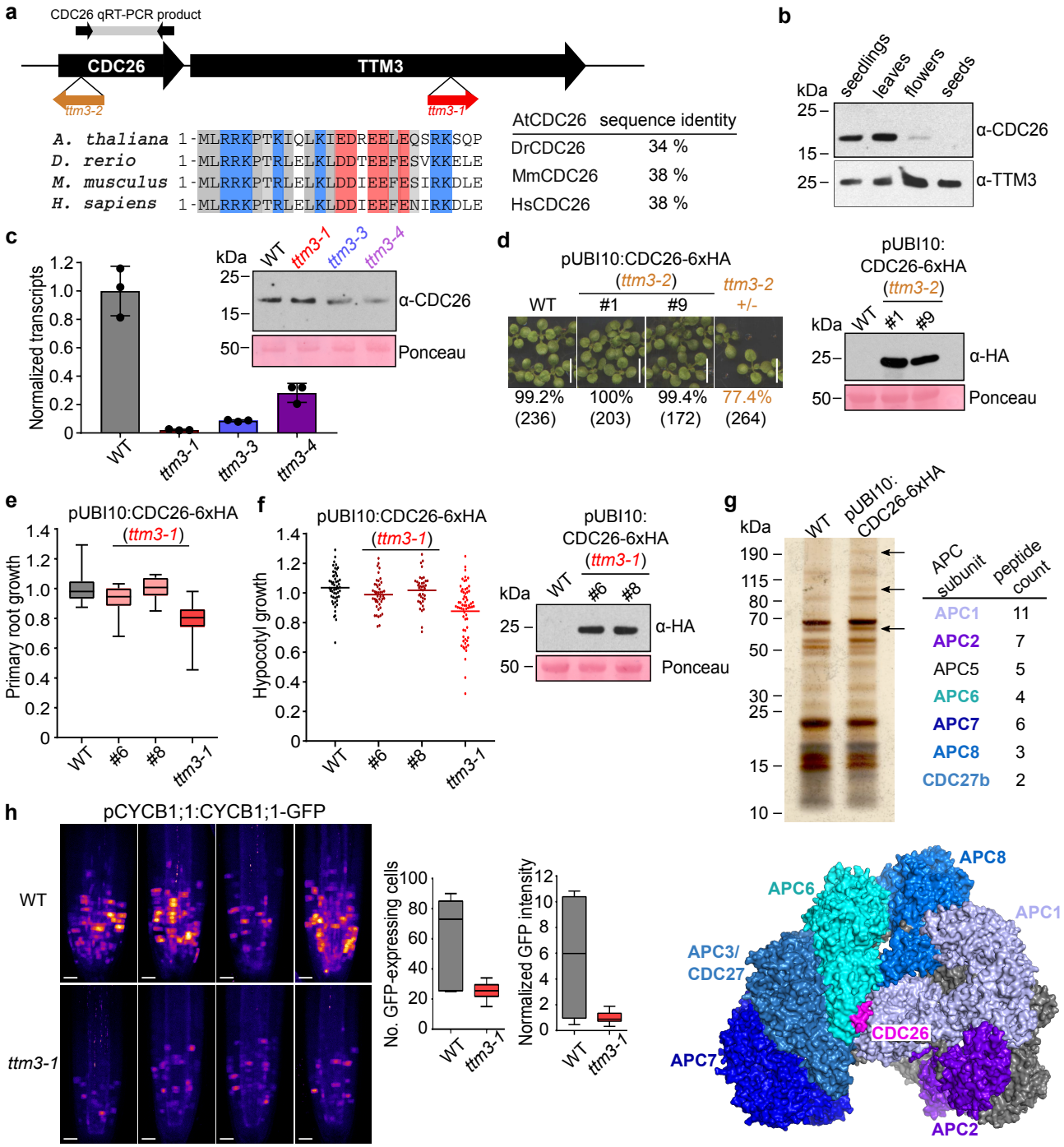
a
CDC26 qRT-PCR product
CDC26
TTM3
ttm3-2
ttm3-1
A. thaliana 1-MLRRKPTKIQLKIEDREELEQSRKSQP
D. rerio 1-MLRRKPTRLELKLDDTEEFESVKKELE
M. musculus 1-MLRRKPTRLELKLDDIEEFESIRKDLE
H. sapiens 1-MLRRKPTRLELKLDDIEEFENIRKDLE
AtCDC26 sequence identity
DrCDC26 34 %
MmCDC26 38 %
HsCDC26 38 %
b
kDa
seedlings
leaves
flowers
seeds
25
15
25
α-CDC26
α-TTM3
c
Normalized transcripts
WT
ttm3-1
ttm3-3
ttm3-4
kDa
25
15
50
α-CDC26
Ponceau
d
pUBI10:CDC26-6xHA
(ttm3-2)
WT
#1
#9
ttm3-2 +/-
99.2% (236)
100% (203)
99.4% (172)
77.4% (264)
pUBI10: CDC26-6xHA (ttm3-2)
kDa
25
50
α-HA
Ponceau
e
pUBI10:CDC26-6xHA
(ttm3-1)
Primary root growth
WT
#6
#8
ttm3-1
f
pUBI10:CDC26-6xHA
(ttm3-1)
Hypocotyl growth
WT
#6
#8
ttm3-1
pUBI10: CDC26-6xHA (ttm3-1)
kDa
25
50
α-HA
Ponceau
g
kDa
WT
pUBI10: CDC26-6xHA
190
115
80
70
50
30
25
15
10
APC subunit
peptide count
APC1 11
APC2 7
APC5 5
APC6 4
APC7 6
APC8 3
CDC27b 2
h
pCYCB1;1:CYCB1;1-GFP
WT
ttm3-1
No. GFP-expressing cells
Normalized GFP intensity
WT
ttm3-1
APC8
APC6
APC1
APC3/ CDC27
CDC26
APC7
APC2

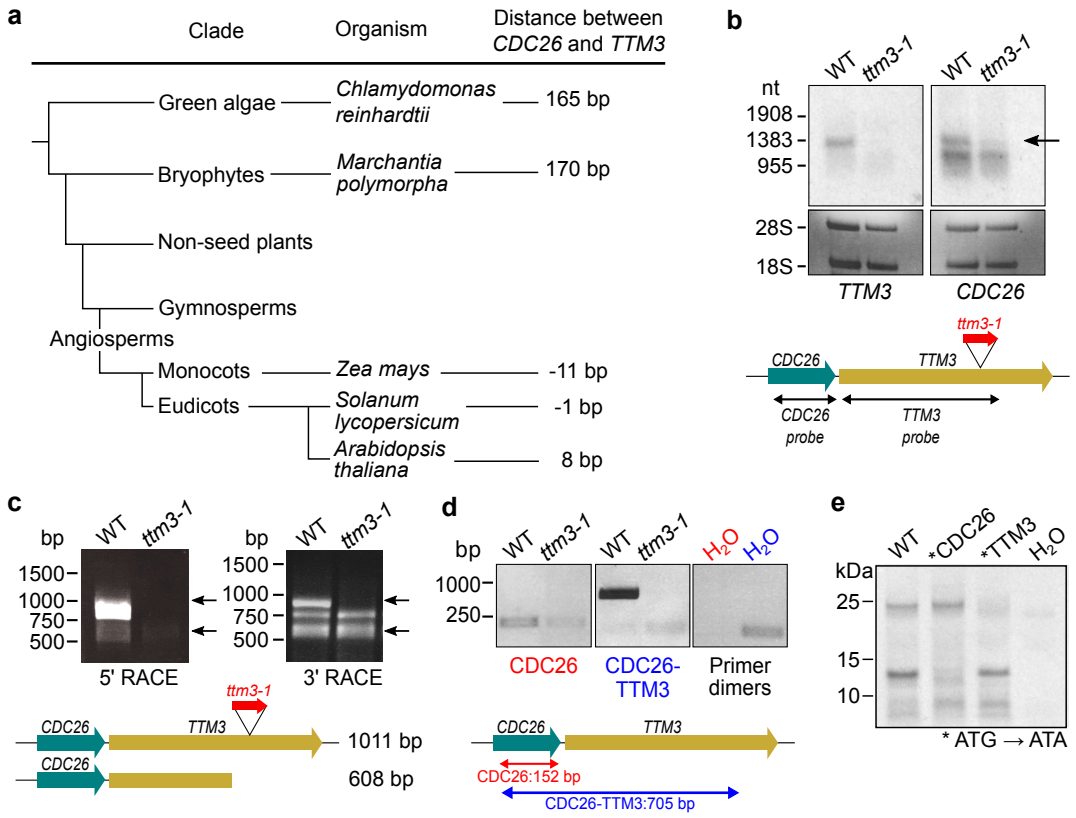
a
Clade
Organism
Distance between CDC26 and TTM3
Green algae
Chlamydomonas reinhardtii
165 bp
Bryophytes
Marchantia polymorpha
170 bp
Non-seed plants
Gymnosperms
Angiosperms
Monocots
Zea mays
-11 bp
Eudicots
Solanum lycopersicum
-1 bp
Arabidopsis thaliana
8 bp
b
WT
ttm3-1
nt
1908
1383
955
28S
18S
TTM3
CDC26
ttm3-1
CDC26
TTM3
CDC26 probe
TTM3 probe
c
bp
1500
1000
750
500
5' RACE
3' RACE
ttm3-1
CDC26
TTM3
1011 bp
608 bp
d
bp
1000
250
CDC26
CDC26-TTM3
Primer dimers
H2O
CDC26:152 bp
CDC26-TTM3:705 bp
e
WT
*CDC26
*TTM3
H2O
kDa
25
15
10
* ATG → ATA

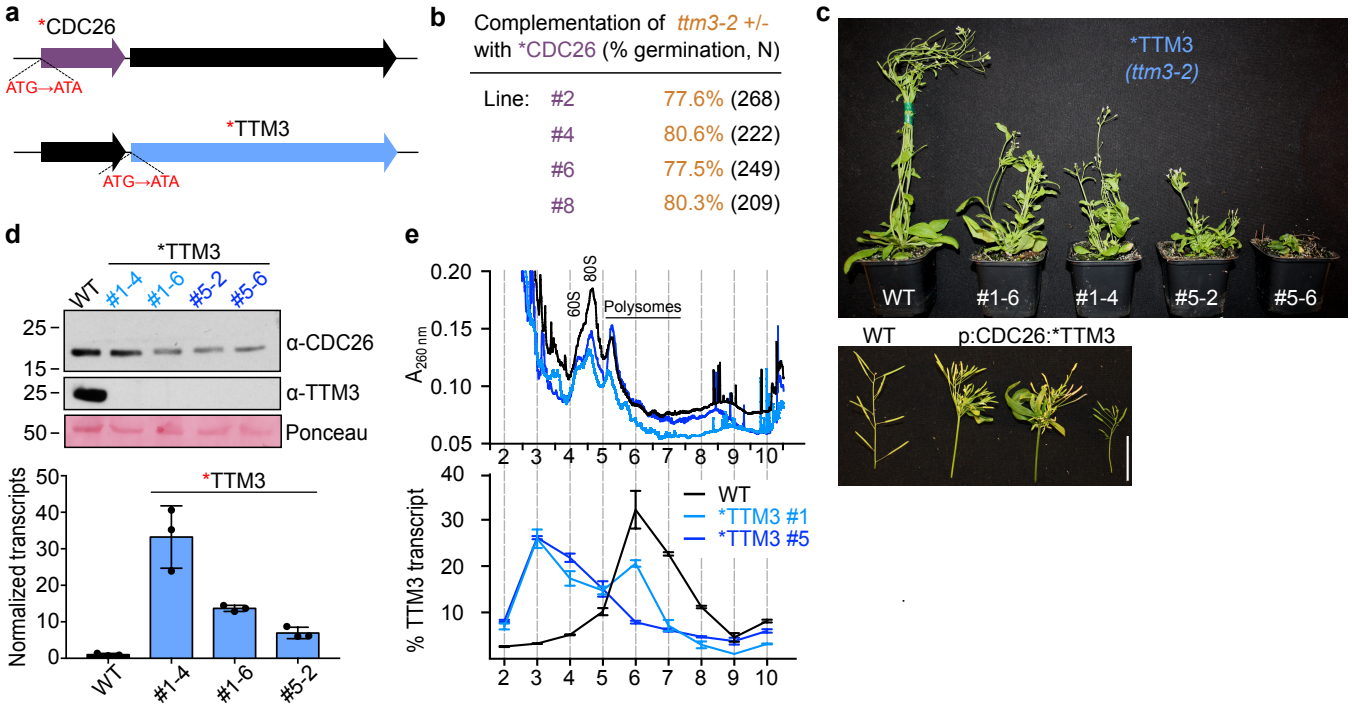
a
*CDC26
ATG→ATA
*TTM3
ATG→ATA
b
Complementation of ttm3-2 +/- with *CDC26 (% germination, N)
Line: #2 77.6% (268)
#4 80.6% (222)
#6 77.5% (249)
#8 80.3% (209)
c
*TTM3
(ttm3-2)
WT
#1-6
#1-4
#5-2
#5-6
WT
p:CDC26:*TTM3
d
*TTM3
WT
#1-4
#1-6
#5-2
#5-6
25
15
25
50
α-CDC26
α-TTM3
Ponceau
Normalized transcripts
*TTM3
WT
#1-4
#1-6
#5-2
e
60S
80S
Polysomes
A260 nm
% TTM3 transcript
WT
*TTM3 #1
*TTM3 #5

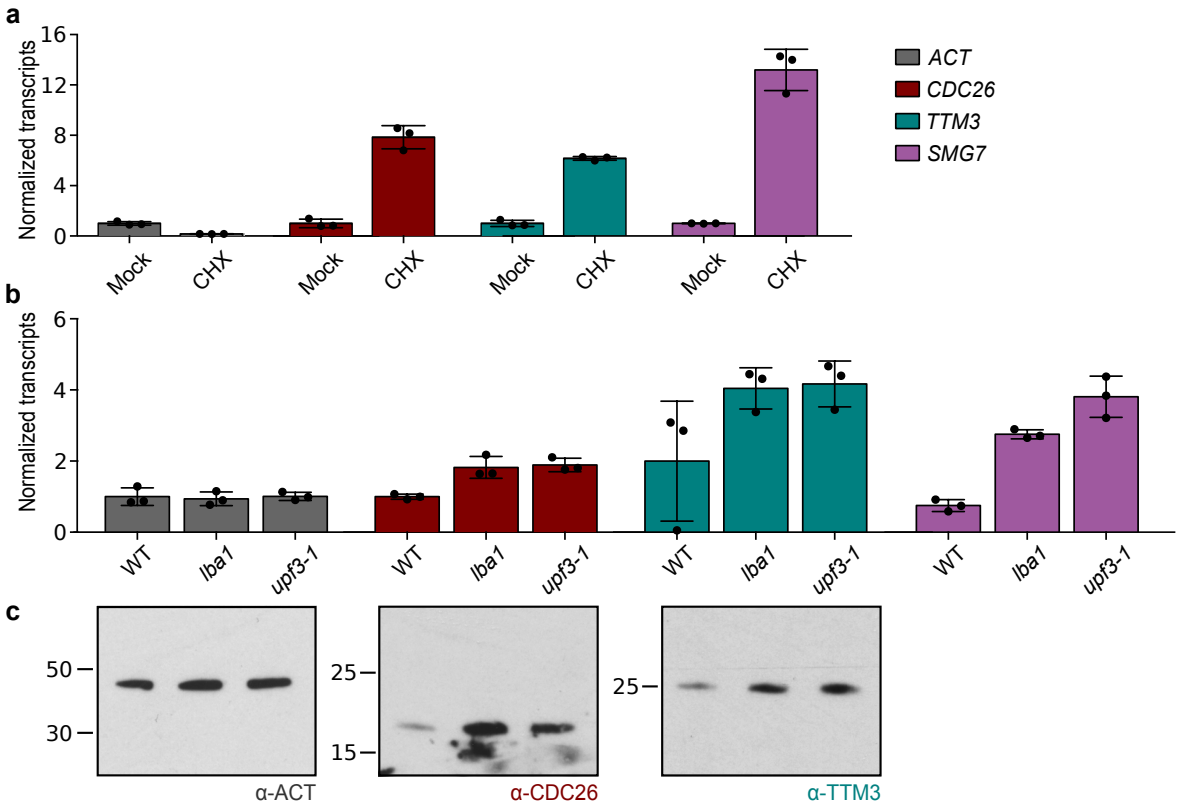
a
Normalized transcripts
16
12
8
4
0
ACT
CDC26
TTM3
SMG7
Mock
CHX
Mock
CHX
Mock
CHX
Mock
CHX
b
Normalized transcripts
6
4
2
0
WT
lba1
upf3-1
WT
lba1
upf3-1
WT
lba1
upf3-1
WT
lba1
upf3-1
c
50
30
α-ACT
25
15
α-CDC26
25
α-TTM3

a

```
CrTTM3     1- MEVEIKIRLPDRAAYEQVAAALAAAPGGKGRLDSHAQGYRMVLVTPTSRCARPHQANYFFDGPNQELNSRRVVLRVRTYDVD---- -82
MpTTM3     1- MEVEVKLKLPGREAHEKVASSLKAF----------------------HEVTHMQENVFFDGANKELSSKRAVLRLRFYNGD---- -59
ZmTTM3     1- MEVEIKLRLPDAAAHRRLSAFLAP----------------------RLRRTHAQRNLFFDDAARTLGAATAALRVRLYDGPDD-- -61
SlTTM3     1- MEVEVKLRLPDSSAHQKVLSLFSS----------------------HHKKTHHQRNTFFDGAAGELSSRRAVLRLRFYENSE--- -60
AtTTM3     1- MEVEVKLRLLTAAAHLRLTTLLTP----------------------YHLKTLHQRNTFFDTPKNDLSLRRAVLRLRFLQNAAVSA -63

CrTTM3    83- -----KKATVTLKGKQILENGIGRASEVEAEVPPAAAAAYLTQPSRML-AEVPIVKDAAEKFGVG----SLVALGGFQNQRDVYEW -158
MpTTM3    60- -----GKCVVTFKGNAVIVDGISRGEELEEDIDVSLGRACVAEPWRLATTTCKLLNKVVADFAC----EDFVCLGGFRNVRTVFNW -136
ZmTTM3    62- --RGPSRAVLALKRRPRIEAGVSRVEEIEEPLEPALAVACADDPARLGGLDSPIIRLVAAEYGVGGDAAPFLCLGGFGNTRAVYEY -145
SlTTM3    61- ----KVKCMVCLKAKAVIIDGVSRVEEDEEELDPKIGYECVSNPRKLMEVDSRVLKRAREEFHVG-E-EGFIGLGGFKNVRNVFEW -140
AtTTM3    64- ASPSPPRCIVSLKAKPTLANGISRVEEDEEEIEYWIGKECVESPAKLSDIGSRVLKRVKEEYGFN-DFLGFVCLGGFENVRNVYEW -148

CrTTM3   159- E------GHTLELDETKFEHGTLYEIEVETEQPEVLRDRLEHWLSGMGVSYSYSQTSKFANFINKTLL- -220
MpTTM3   137- E------GLKIELDETQYDFGTTYEVECESTDPERVREVLGDFLKSKGIEFTYSTKSKFAVFRSGKIE- -198
ZmTTM3   146- ELEDGGGGLVLELDETRFDFGTRYELECETAEPDRVKEVLERLLTVAGVPYEYCRNSKFACFMTGKLLP -214
SlTTM3   141- C------GVELEVDETMYDFGTFYEIECESLEPEKVKAMIEAFLKDNDIDYSYSEVSKFATFRAGKLP- -202
AtTTM3   149- R------GVKLEVDETKYDFGNCYEIECETEEPERVKTMIEEFLTEEKIEFSNSDMTKFAVFRSGKLP- -210
```

AtTTM3	sequence identity
CrTTM3	39 %
MpTTM3	47 %
ZmTTM3	45 %
SlTTM3	59 %

b

deleted in *ttm3-3*

```
TTM      1 - ATGGAAGTCGAAGTCAAGCTCCGTCTCCTAACCGCCGCTGCTCATCTCCGTCTCACCACTCTCCTCACTCC(...)TGA - 633
ttm3-3   1 - ATGGAAGTCGAAGTCAAGCTCC                TGCTCATCTCCGTCTCACCACTCTCCTCACTCC(...)TGA - 617

TTM      1 - MEVEVKLRLLTAAAHLRLTTLLTPYHLKTLHQRNTFFDTPKNDLSLRRAVLRLRFLQNAAVSAASPSPPRCIVSLA(...)KLP - 210
ttm3-3   1 - MEVEVKLLLISVSPLSSLHTTSKPFTNATPSSTHPKTTSLSAAPSSVSASFKTPPFPRLLLLRRVVSSLLKRSQL          - 75
```

Supplementary Fig. 1 | TTM3 is conserved among different plant species. a, Multiple sequence alignment of different TTM3 orthologs from *Arabidopsis thaliana* (Uniprot ID Q9SIY3), the green algae *Chlamydomonas reindhartii* (Uniprot ID A8J8R5), the bryophyte *Marchantia polymorpha* (Uniprot ID A0A176WD54) and the angiosperms *Zea mays* (Uniprot ID B6TQK5) and *Solanum lycopersicum* (NCBI ID XP_004242731.1). Sequence fingerprints of the CYTH-like protein superfamily are highlighted in cyan, invariant amino-acids are shown in yellow. **b**, The *ttm3-3* mutant harbors a 16 base pair deletion in the *TTM3* coding sequence (highlighted in red). Translation of the *ttm3-3* mutant allele would result in a truncated protein of 75 amino-acids, with severely altered amino-acid sequence.

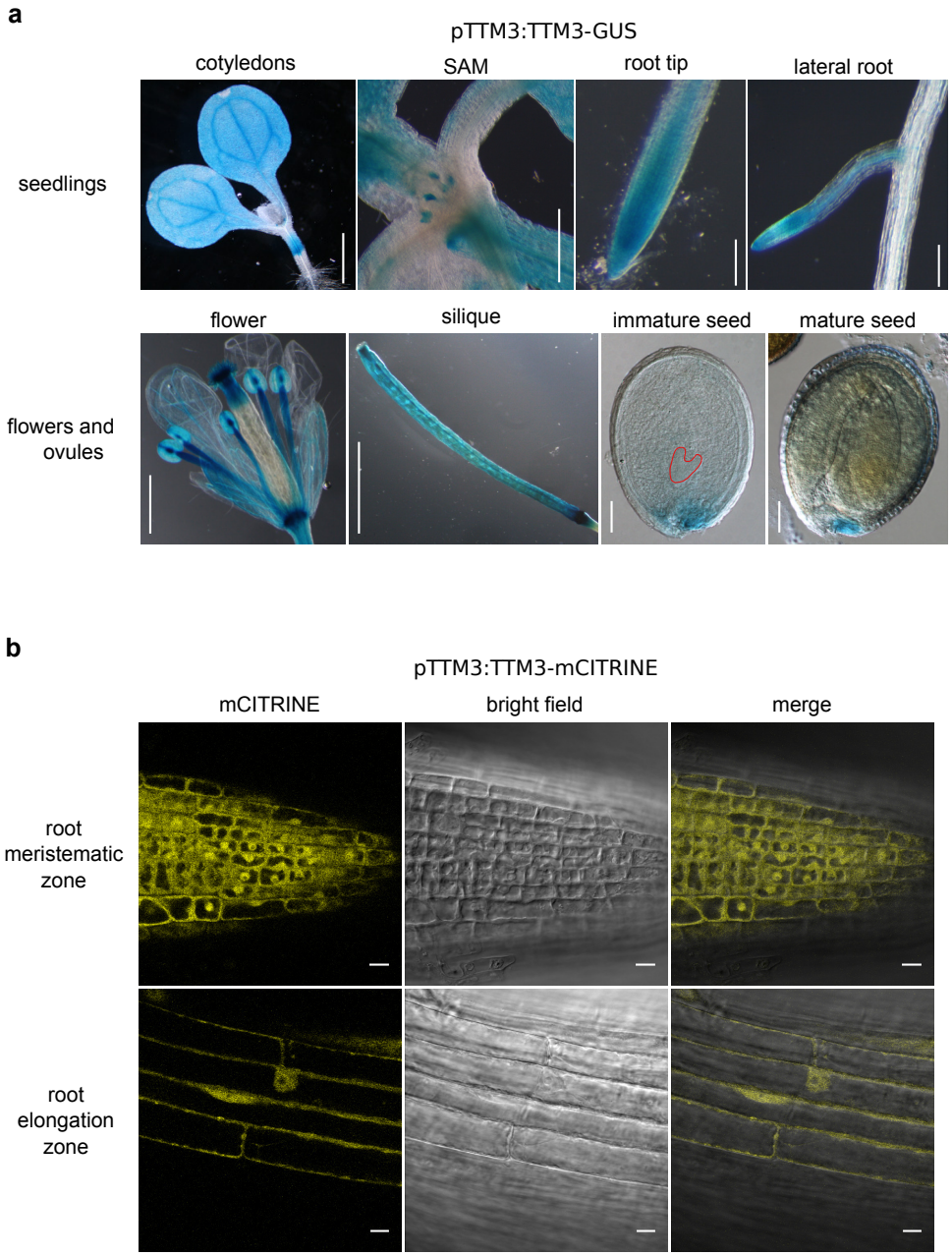

Supplementary Fig. 2 | TTM3 is a nuclear/cytosolic protein expressed in different tissues in Arabidopsis. a, Wild-type seedlings expressing TTM3-GUS, under the control of the endogenous *TTM3* promoter and including the annotated 5' UTR, reveal TTM3 expression in hypocotyl, cotyledons, the shoot apical meristem (SAM), root tips and lateral roots. In flowers, TTM3-GUS is restricted to the abscission zone, stamens, stigma and petal vasculature. In seeds, GUS staining is found in the chalazal endosperm and testa. Scale bars: 0.05 mm in seeds, 0.5 mm in siliques, flowers and SAM, 1 mm in roots and cotyledons. Experiments were performed 4 times, with similar results. **b**, Wild-type seedlings expressing TTM3-mCITRINE, under the control of the endogenous *TTM3* promoter and including the 5' UTR, revealed TTM3-mCITRINE localized in the nucleus and cytosol of root cells (scale bars: 10 µm). Three independent transgenic lines expressing pTTM3:TTM3-mCITRINE showed a similar fluorescent pattern. A western blot showing accumulation of the TTM3-mCITRINE fusion protein in these lines is shown in Fig. 2e.

a

> *C. reinhardtii*

CRgenome|CrChr16[1870194-1870688]

-492

ATGCTGCCGCGCAAGCCTACTCGCATAGATCTCAAGCCAGCGGACAAGGAAGAGGTCAGAACTCTGCTCTGGGACCTGGCTGTTCGCGCGTCGATTCCATTA
TTTGGGGTTCGCTATACGACAGCCATTTCTCCTTCCCTTGCTCCTACAGTACGAGAACCTCAAAGCTTTACAGCTGGAGCGCAAAGCGGCCCTGGAGCACGC
TTCGGACGCGTTCTTGCCCGATCCTCTCCAGGTCCGCCGCGGCGGGGGTTGGGACCCAACGATTGCAGGGGTGCGGGTCGAGGGATGGCGCATAGGTTATCT
AGAACAGTTGCAGCGGTCTGAGAGGCCCTGTGCGGGGCGGCCGGGCACCACACACACCCGCCTCTTCCCCTACCCCATCTGCGCGCGACTCTAAACCACCCC
TCATACCTTGACCCCGCCTGCCGGTGTGCCGCAGGTGGAGAAGCGCTCCACGGCGGCGCGGATAGGCCTGCGGAAGTGAGGCCCATG

+1

> *M. polymorpha*

scaffold00152[209114-209505]

-389

ATGTTGAAGAGGAAGCCGACGAGGCTCGAGTTCAAGGAGGCCGATGACAAGGAGGATCTAGAGCAAGCACGGAAGAGCGCATCTGCTGCCGCCGCTGCTGCT
GCTGCGGCTTCGTCTGCAGGTGCTGCTGCCGTTGGTGGCTCTGCTTCTGCTACCCCGCAAGTCATCGAATTTCGCCCTAAACTTTCTGTCGCTCAACGAATA
GGATTCAACAAGTAGTTGTGCTGCAGCGTGTGAATTTTGTGGGTGCGGGCCCGCACGCCGTTGCGCAAGGCGTGGCCGAGTGGTGGTGTGGTGGTACTTTCC
CTTGGTGTTTGTACATTGGACTGGGTTAATAAATTTTGCTCGGACTGCAAGAGAGTGGCGGTTTGTTCTCTTCGGTTCTCGGAATG

+1

> *Z. mays*

NW_007617763.1:174002602-174002886 Zea mays cultivar B73 chromosome 7 genomic scaffold, B73 RefGen_v3
7

-274

ATGCTGCGCCGCAACCCAACCCatgctgcgccgcaaGCATCGAGCTCACCTCCTCCGACCGCGACGAGCTCGAAGACCACCTCCGCGCCGCCGCGGCAGCCA
CCACCACCAAGGATCCTTCCGGTTACACCACTCCGTCTCCAGTCCTTGGCCCGCAGACCTCCAATCCCCTGCTCCAATTCCTCCACCCGAAGCCCGGCGCCG
TGCCATCCAAGTCCCAACGCATCGGCATCGGCCTCTCCACCCCGCCGGCTCCGGCCCCGAACCCGCGACCACCCCATCCACCCCATGGAGGTTGA

+1

> *S. lycopersicum*

SL3.0ch07[2203432-2203209]

-221

ATGCTGAGAAGAAAGCCCAGCAAAATCGAAGTAAAAATCGAAGACAAAGAAGAACTCGAAGAAGCTCGCAAACGCGCCGCCCTCATCGCCGCCTCTTCCTCC
ACCAGTACCGCCGCCGGTACCGGCGGAGCTGCCACAGCCGGTGTCTCCTCTCTCCTCCAACACTTCGACCGATCAACAGTCGATCCTTCCTCCAAAAACAAC
CGCATCGGCCTCAATTAATG

+1

> *A. thaliana*

Chr2[4802793-4803002]

-206

ATGTTGAGAAGAAAACCAACAAAAATCCAACTCAAAATCGAAGACCGTGAAGAGCTTGAACAATCCCGCAAATCTCAACCATCCACCACCACAACCACCGCA
CCATCTTCCTCCTCCGCCGCCTCCTCTCTCCACCACCTCATAGACCCAAAACACAAAAACCCTTCCTCCAAATCCGACCGAATCGGTCTCTCTTAAAACACT
CCATG

+1

b

Organism	cDNA clone (sequence ID)	length
C. reinhardtii	XM_001697825.1	2039 bp
Z. mays	BT037955.1	1237 bp
S. lycopersicum	AK321570.1	1134 bp
A. thaliana	AK316974.1	949 bp

c

ANAPC_CDC26 motif

```
C. reinhardtii   1- MLPRKPTRIDLKPA-DKEEVRTLLWDLAVRASIP----------LFGVRYTTAISPSLAPTVREPQSFTAGA -61
M. polymorpha    1- MLKRKPTRLEFKEADDKEDLEQARKSASAAAAAAAAASSAGAAAVGGSASATPQVIEFRPK----------- -61
Z. mays          1- MLRRNPTRIELTSS-DRDELEDHLRAAAAATTTKDPSGYTTPSPVLGPQTSNPLLQFLHPKPGA-------- -63
S. lycopersicum  1- MLRRKPSKIEVKIE-DKEELEEARKRAALIAASSSTSTAAGTGG-AATAGVSSLLQHFDRSTVD-------- -62
A. thaliana      1- MLRRKPTKIQLKIE-DREELEQSRKSQPSTTTTT--------AP-SSSSAASSLHHLIDPKHKN-------- -54

C. reinhardtii  62- QSGPGARFGRVLAR--------SSPGPPRRGLGPNDCRGAGRGMAHRLSRTVAAV -108
M. polymorpha   62- -LSVAQRIGFNK------------------------------------------ - 72
Z. mays         64- VPSKSQRIGIGLSTPPAPAPNPRPPHPPHGG------------------------ - 94
S. lycopersicum 63- PSSKNNRIGLN----------------------------------------- - 73
A. thaliana     55- PSSKSDRIGLS----------------------------------------- - 65
```

AtCDC26	prot id
CrCDC26	25 %
MpCDC26	39 %
ZmCDC26	40 %
SlCDC26	46 %

Supplementary Fig. 3 | CDC26 transcript and protein sequences are conserved across the entire plant lineage. a, The *CDC26* ORF (in blue) is located upstream of *TTM3* (initiation codon in red) in the green algae *Chlamydomonas reindhartii* (CR genome database: http://www.plantgdb.org/CrGDB), the bryophyte *Marchantia polymorpha* (MP genome database: http://marchantia.info/genome) and the angiosperms *Zea mays* (NCBI reference: NW_007617763.1), *Solanum lycopersicum* (SGN database: https://solgenomics.net/) and *Arabidopsis thaliana* (Araport11: https://www.arabidopsis.org). **b**, Table summary of existing cDNA clones containing *CDC26* and *TTM3* ORFs from different species, and including the respective NCBI identifiers (https://www.ncbi.nlm.nih.gov/genbank/). **c**, The predicted CDC26 protein sequences (translated from *CDC26* CDS) are conserved among different plant species. The CDC26 motif is shown in gray.

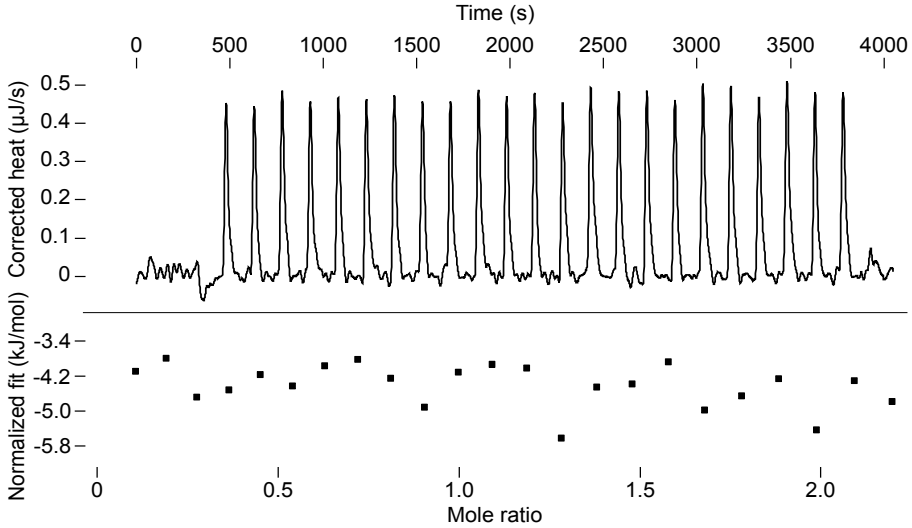

Supplementary Fig. 4 | Isothermal titration calorimetry (ITC) of recombinant CDC26 versus TTM3. CDC26 at a concentration of 200 µM was injected into a 50 µM TTM3 solution in the cell (10 µL per injection, 25 injections in total, 150s intervals). No heats were detected, suggesting that CDC26 and TTM3 show no detectable binding in this assay.

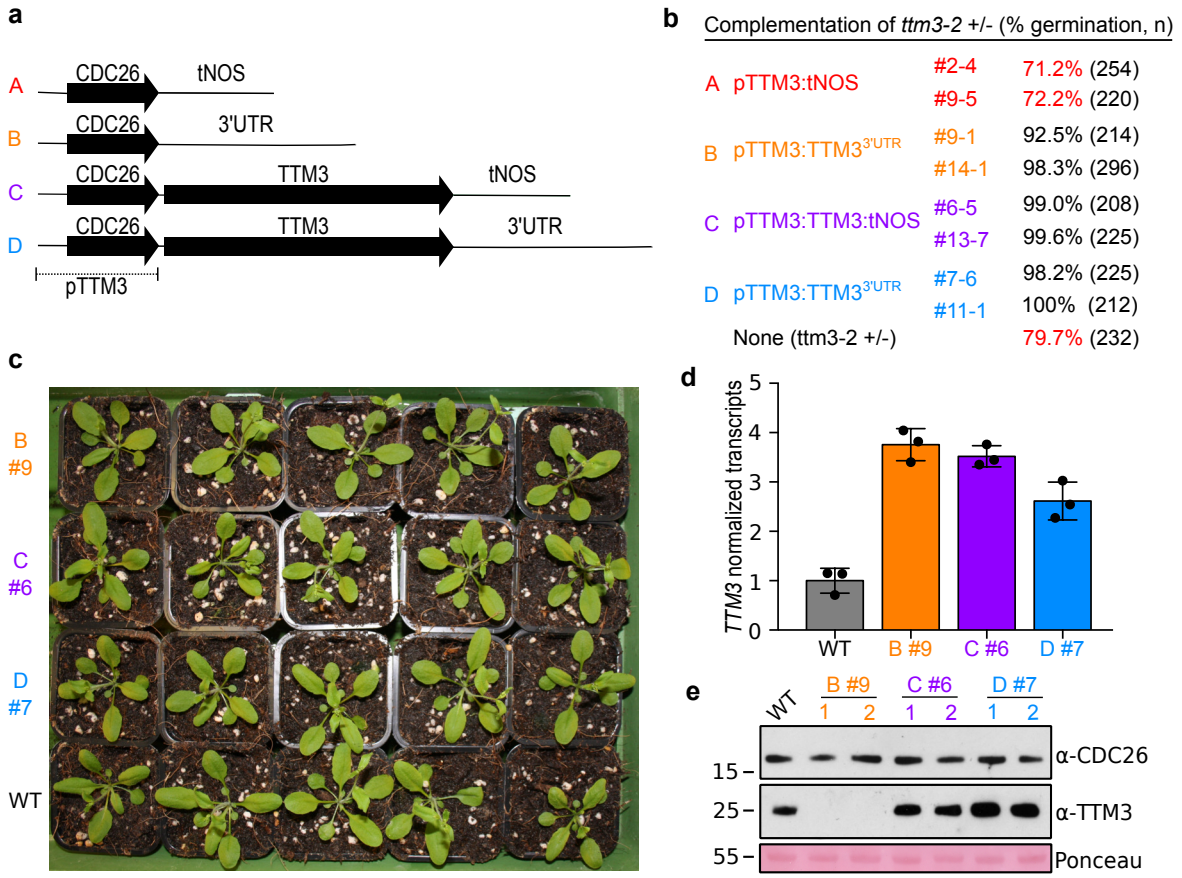

Supplementary Fig. 5 | Genetic analysis of the *CDC26-TTM3* bicistronic transcript indicates a role for the *TTM3* mORF and the 3' UTR in *CDC26* expression. a, Schematic representation of the constructs used to complement *ttm3-2* heterozygous plants. **b,** Complementation of *ttm3-2* requires the presence of either the *TTM3 m*ORF or the *TTM3* 3'UTR when expression is driven by the endogenous promoter. Constructs were transformed to heterozygous *ttm3-2* plants and complementation was assessed in seed germination assays. Shown are germination rates, with the total number of seeds analyzed shown in brackets. Two independent transgenic lines (indicated with #) were analyzed per construct. **c,** 4 week-old homozygous *ttm3-2* plants complemented with *CDC26* harboring the *TTM3* 3'UTR or with the bicistronic *CDC26– TTM3* transcript display wild-type-like phenotypes (experiment was repeated more than twice with 2 independent transgenic lines, only one representative line is shown). **d,** *CDC26* transcript levels, measured by qPCR (primer sequences CDC26_RT_F/R, see Supplementary Table 2) from complemented lines shown in panel c. Shown are mean values ± SD, n=3 technical replicates (experiment repeated twice with similar results). **e,** CDC26 protein levels are similar to wild-type, while TTM3 levels are higher in plants containing the *TTM3* 3'UTR. Western blots were performed using leaf tissue from 2 independent plants, and repeated twice with similar results.

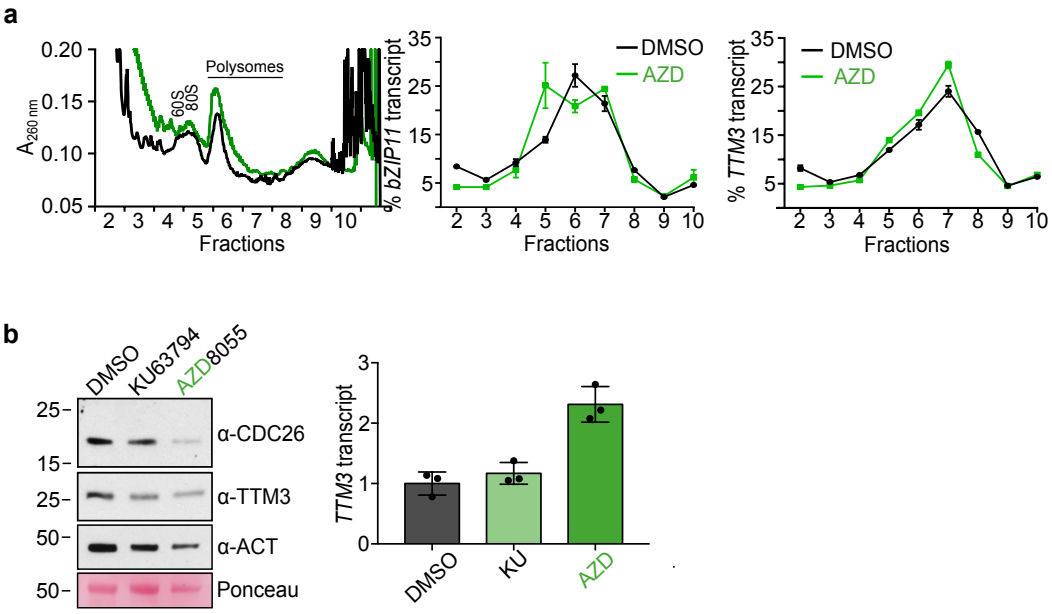

Supplementary Fig. 6 | CDC26 and TTM3 translation is TOR-independent. a, Polysome profiles of wild-type seedlings treated for 4 h with the TOR-inhibitor AZD8055 (AZD) show changes for *bZIP11*, but not for *TTM3* transcript levels. cDNA was extracted from ~20 seedlings per treatment, and the experiment was performed twice with similar outcome. Shown are mean values ± SD, n=3 technical replicates. **B**, 4 d old seedlings treated for 3 d with 3 µM TOR-inhibitors show a reduction in CDC26 and TTM3 protein levels comparable to actin (left), as seen in 2 independent experiments. *TTM3* mRNA levels (obtained from ~20 seedlings per treatment) are equal or higher upon treatment (right, primer sequences TTM3_RT_F/R in Supplementary Table 2).

a

```
CDC26 WT          1- ATGTTGAGAAGAAAACCAACAAAAATCCAACTCAAAATCGAAGACCGTGAAGAGCTTGAACAATCCCGCAAATCT -74
CDC26alt.codons   1- ATGCTGCGCCGGAAACCCACGAAAATACAACTGAAAATTGAAGATCGGGAGGAGTTGGAACAGTCGAGAAAGAGC -74
                        *  * ** *     *  *     *     *     *     *  *  *   * **    *  ** *  ****

CDC26 WT         75- CAACCATCCACCACCACAACCACCGCACCATCTTCCTCCTCCGCCGCCTCCTCTCTCCACCACCTCATAGACCCA -149
CDC26alt.codons  75- CAACCCTCCACTACGACTACAACCGCACCCTCCTCTTCGAGCGCGGCATCATCACTGCATCATTTAATCGACCCT -149
                           *     *  *  *  *         *  *  *  ***   *  *  *  *  *  *  ** *  *     *

CDC26 WT        150- AAACACAAAAACCCTTCCTCCAAATCCGACCGAATCGGTCTCTCTTAA -198
CDC26alt.codons 150- AAACATAAGAACCCGAGTTCTAAGAGTGACAGAATTGGGCTGAGCTAA -198
                        *  *     * **  *  ****   *    *  *  ****
```

b

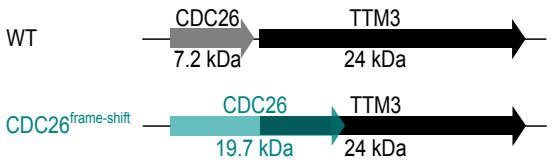

c

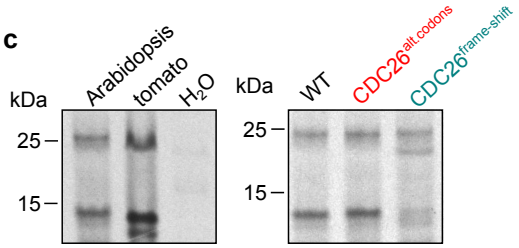

Supplementary Fig. 7 | CDC26 and TTM3 can be translated in wheat germ extract independently of *CDC26* uORF sequence and length. a, DNA sequence of a synthetic construct in which 32% of *AtCDC26* coding sequence has been replaced by alternative codons ($CDC26^{alt.codons}$). Shown is a sequence alignment with the wild-type AtCDC26 sequence (the * denotes non-identical nucleotides). **b,** Deletion of cytosine in position +187 of *CDC26* uORF ($CDC26^{frameshift}$) results in a C-terminally extended CDC26 variant, which is ~12 kDa larger than wild-type CDC26. **c**, *In vitro* translation of wild-type Arabidopsis and tomato *CDC26-TTM3* transcripts yields two protein products (left panel). $CDC26^{alt.codons}$ and $CDC26^{frameshift}$ are efficiently translated as well in wheat germ extracts (right panel). Experiments were performed twice with similar results.

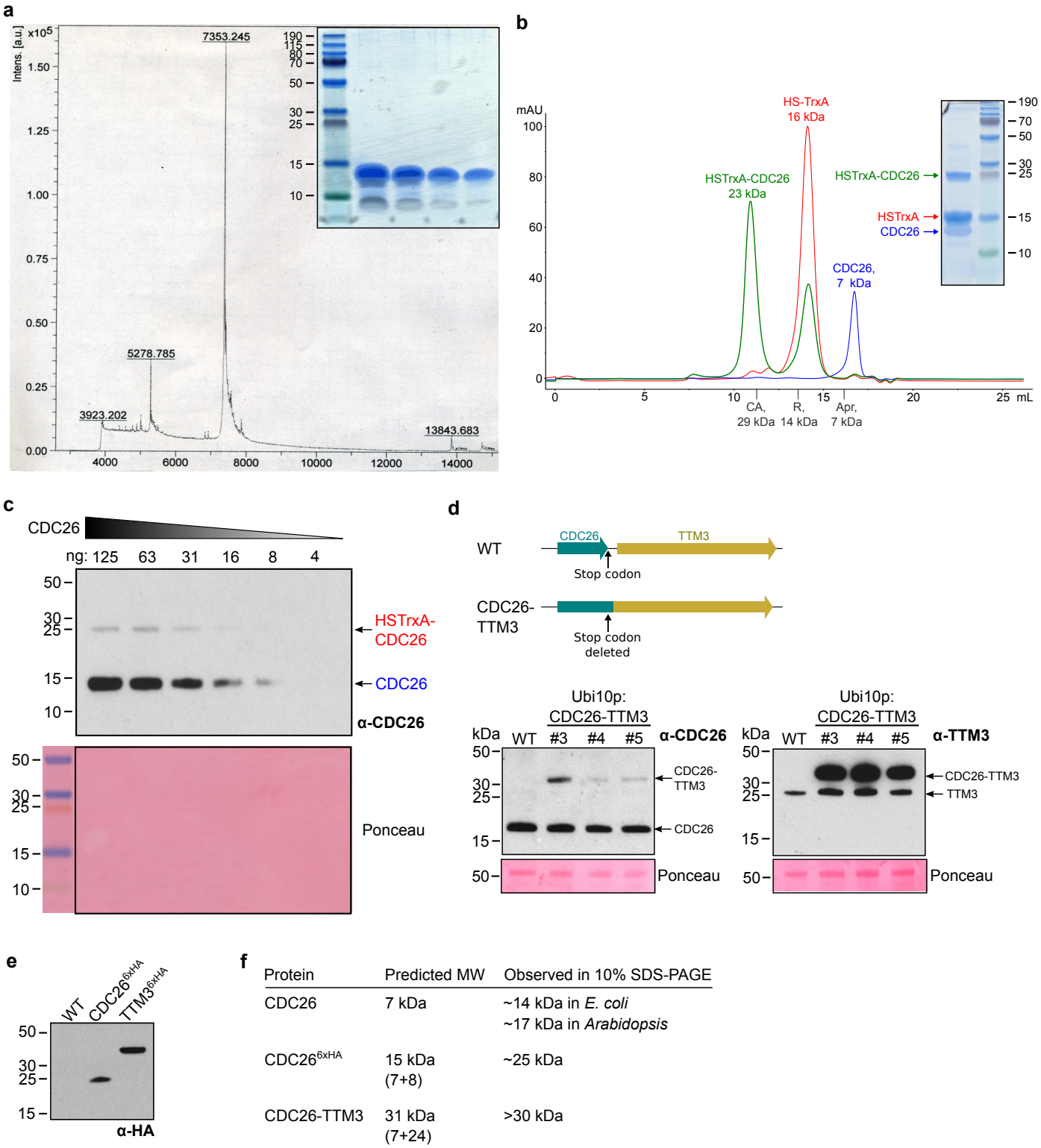

f

Protein	Predicted MW	Observed in 10% SDS-PAGE
CDC26	7 kDa	~14 kDa in *E. coli* ~17 kDa in *Arabidopsis*
CDC26^{6xHA}	15 kDa (7+8)	~25 kDa
CDC26-TTM3	31 kDa (7+24)	>30 kDa

Supplementary Fig. 8 | Characterization of the polyclonal CDC26 antibody. a, Recombinant CDC26 produced in *E. coli* migrates as a ~ 14 kDa protein in 12% SDS-PAGE (top right). MALDI-TOF mass spectrometry analysis reveals a native molecular weight (MW) of ~ 7.3 kDa for AtCDC26 (theoretical MW: 7339.2 Da). Experiment performed twice with similar results. **b**, CDC26 migrates as a ~ 7 kDa protein in analytical size-exclusion chromatography (Superdex 75 10/300 GL). MW standards: aprotinin (Apr), RNAse A (R), carbonic anhydrase (CA) and conalbumin (C). Experiment performed twice with similar results. A 12 % SDS-PAGE is shown alongside. **c**, Western blot of recombinant CDC26 using the anti-CDC26 antibody detects CDC26 (running at ~ 14 kDa, as shown in panel b) and residual amounts of the thioredoxin (TrxA)-CDC26 fusion protein not completely digested during TEV cleavage (running at ~ 23 kDa as shown in panel b, see Methods). Experiment performed twice with similar results. **d**, Deletion of the CDC26 stop codon results in a CDC26-TTM3 fusion protein (MW: 31 kDa) that can be detected by western blot using both anti-CDC26 and anti-TTM3 antibodies. Experiment performed twice with similar results. **e**, The 6xHA tag adds ~8 kDa to CDC26 and TTM3 fusion proteins expressed under the control of the *UBI10* promoter in Arabidopsis transgenic lines. Western blot using an anti-HA antibody detects TTM3-6xHA at ~ 35 kDa and CDC26-6xHA at ~ 25 kDa. Experiment performed 3 times with similar results. **f**, Table summarizing the predicted MW of CDC26 and CDC26-fusion proteins *versus* the actual observed sizes in SDS-PAGE.

Supplementary Table 1| Arabidopsis transgenic lines generated for this study.

Construct	Background	Vector	Resistance
pTTM3*:TTM3-GUS	Col (WT)	pH7m34GW	Hyg
pTTM3*:TTM3-mCITRINE	*ttm3-1*	pB7m34GW	Basta
pTTM3*:TTM3-mCITRINE	*ttm3-2*	pH7m34GW	Hyg
pTTM3*:TTM3$^{[E2AE4AE169A]}$:mCITRINE	*ttm3-2*	pH7m34GW	Hyg
pTTM3*:TTM3$^{[R52A]}$:mCITRINE	*ttm3-2*	pH7m34GW	Hyg
pUBI10:CDC26-6xHA	*ttm3-1*	pH7m34GW	Hyg
pUBI10:CDC26-6xHA	*ttm3-2*	pH7m34GW	Hyg
pUBI10:CDC26-6xHA	Ws-4 (WT)	pH7m34GW	Hyg
pTTM3*:TNOS	*ttm3-2* +/-	pGIIH	Hyg
pTTM3*:TTM3$^{3'UTR}$**	*ttm3-2*	pGIIH	Hyg
pTTM3*:TTM3:tNOS	*ttm3-2*	pGIIH	Hyg
pTTM3*:TTM3:TTM3$^{3'UTR}$**	*ttm3-2*	pGIIH	Hyg
pTTM3*[CDC26$^{[ATG\rightarrow ATA]}$]:TTM3	*ttm3-2* +/-	pH7m34GW	Hyg
pTTM3*:TTM3$^{[ATG\rightarrow ATA]}$	*ttm3-2*	pH7m34GW	Hyg

* pTTM3 refers to *TTM3* endogenous promoter and *TTM3* 5'UTR (*CDC26*), and includes 1035 base pairs located upstream of *TTM3* start codon. ** TTM3$^{3'UTR}$ includes 429 base pairs located downstream of *TTM3* stop codon.

Supplementary Table 2 | Primers used in this study.

Primer name	Purpose	Sequence
ttm3-1_WT_F	Genotyping	GAAGTCGAAGTCAAGCTCCGTCTC
ttm3-1_WT_R	Genotyping	GCTAACCACAGAGATTAAGAAAGACTTAC
ttm3-1_T-DNA_R	Genotyping	TGGTTCACGTAGTGGGCCATCG
ttm3-2_WT_F	Genotyping	CCCTTGTTTTATGAACATTGGATCACA
ttm3-1_WT_R	Genotyping	GCTAACCACAGAGATTAAGAAAGACTTAC
ttm3-1_T-DNA_F	Genotyping	GGAGAAAGATGAGGGTTAAGAAACG
ttm3-1_T-DNA_R	Genotyping	CGTGTGCCAGGTGCCCACGGAATAGT
ttm3-3_seq_R	Genotyping	CATCTTCCTCCACACGACTAATCCC
CDC26probe_F	Northern blot	AAATCGAAGACCGTGAAGAG
CDC26probe_R	Northern blot	GATTCGGTCGGATTTGGAG
TTM3probe_F	Northern blot	GAAGTCGAAGTCAAGCTCCGTCTC
TTM3probe_R	Northern blot	ACACGCTCTGGTTCCTCTGT
RACE_SP1	RACE	CGAAGAAATGTTGAGAAGAAAACC
RACE_SP2	RACE	GAGAAGAAAACCAACAAAAATCC
RACE_SP3	RACE	CAAAAATCCAACTCAAAATCGAAG
AP	RACE	GGCCACGCGTCGACTAGTACTTTTTTTTTTTTTTTTT
AUAP	RACE	GGCCACGCGTCGACTAGTAC
TTM3_3'_F	RACE	GATTGAATGTGAGACAGAGGAACCAGAG
ATG-ATA_CDC26_sdmF	In vitro translation	CCCTTATATTGAGAAGAAAACCAACAAAAATCCAACTC
ATG-ATA_CDC26_sdmR	In vitro translation	CTTCTCAATATAAGGGCGAATTCGACCCAGCTTTCTTG
ATG-ATA_TTM3_sdmF	In vitro translation	CACTCCATAGAAGTCGAAGTCAAGCTCCGTCTCCTAACC
ATG-ATA_TTM3_sdmR	In vitro translation	GACTTCTATGGAGTGTTTTAAGAGAGACCGATTCGGTCG
CDC26_RT_F	qRT-PCR	AAATCGAAGACCGTGAAGAG
CDC26_RT_R	qRT-PCR	GATTCGGTCGGATTTGGAG
TTM3_RT_F	qRT-PCR	AGTCACCGGCTAAGCTCTCA
TTM3_RT_R	qRT-PCR	ACACGCTCTGGTTCCTCTGT
SMG7_RT_F	qRT-PCR	ACTTGGTCGAGTCGTCACTT
SMG7_RT_R	qRT-PCR	AAGAAGCCAAGGCCACAAAG
ACT8_RT_F	qRT-PCR	GACTCAGATCATGTTTGA
ACT8_RT_R	qRT-PCR	CCAGAGTCCAACACAATA

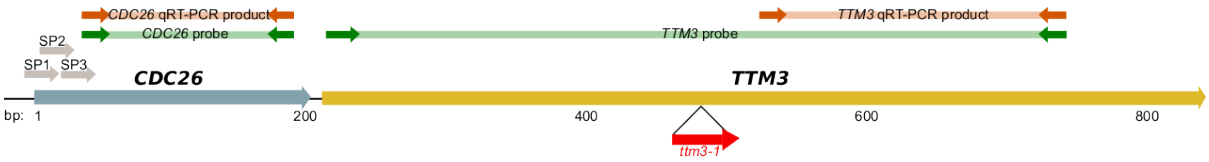

Supplementary data 1. Sequencing results from 5'RACE. Pages 1-3 correspond to a *CDC26-TTM3* bicistronic transcript, including 197 bp downstream of *TTM3*. Pages 4-6 indicate a shorter transcript, covering the complete *CDC26* ORF and only part of the *TTM3* ORF. RACE_SP3 was used as a specific primer for the reaction (see Supplementary Table 2). *CDC26* ORF is marked in blue, *TTM3* ORF in yellow.

CDC26-TTM3 bicistronic transcript

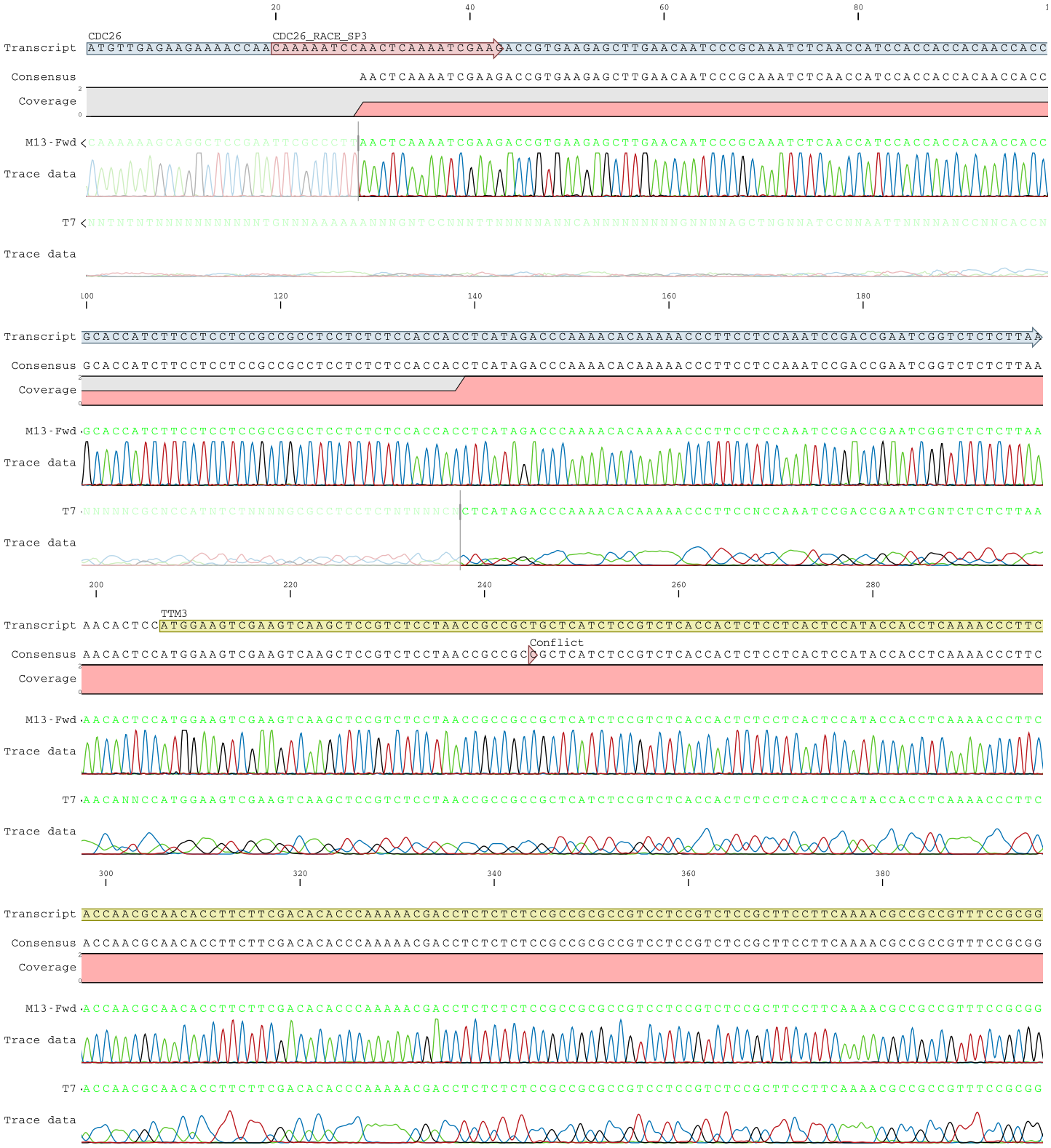


400
420
440
460
480
Transcript CTTCTCCTTCTCCGCCGCGTTGTATCGTCTCTCTTAAAGCGAAGCCAACTCTAGCTAATGGGATTAGTCGTGTGGAGGAAGATGAAGAGGAGATTGAGT
Consensus CTTCTCCTTCTCCGCCGCGTTGTATCGTCTCTCTTAAAGCGAAGCCAACTCTAGCTAATGGGATTAGTCGTGTGGAGGAAGATGAAGAGGAGATTGAGT
Coverage
M13-Fwd CTTCTCCTTCTCCGCCGCGTTGTATCGTCTCTCTTAAAGCGAAGCCAACTCTAGCTAATGGGATTAGTCGTGTGGAGGAAGATGAAGAGGAGATTGAGT
Trace data
T7 CTTCTCCTTCTCCGCCGCGTTGTATCGTCTCTCTTAAAGCGAAGCCAACTCTAGCTAATGGGATTAGTCGTGTGGAGGAAGATGAAGAGGAGATTGAGT
Trace data
500
520
540
560
580
Transcript ATTGGATTGGTAAAGAATGTGTTGAGTCACCGGCTAAGCTCTCAGATATTGGATCTAGGGTTTTGAAAAGGGTTAAAGAGGAATATGGGTTTAATGACT
Conflict
Consensus ATTGGATTGGTAAAGAATGTGTTGAGTCACCGGCTAAGCTCTCAGATATTGGATCTAGGGTTTTGAAAAGGGTTAAAGGGGAATATGGGTTTAATGACT
Coverage
M13-Fwd ATTGGATTGGTAAAGAATGTGTTGAGTCACCGGCTAAGCTCTCAGATATTGGATCTAGGGTTTTGAAAAGGGTTAAAGGGGAATATGGGTTTAATGACT
Trace data
T7 ATTGGATTGGTAAAGAATGTGTTGAGTCACCGGCTAAGCTCTCAGATATTGGATCTAGGGTTTTGAAAAGGGTTAAAGGGGAATATGGGTTTAATGACT
Trace data
600
620
640
660
680
Transcript TTTTAGGGTTTGTTTGTTTAGGTGGCTTTGAGAATGTTAGGAATGTTTATGAGTGGAGAGGTGTTAAACTTGAGGTTGATGAGACTAAGTATGATTTTG
Consensus TTTTAGGGTTTGTTTGTTTAGGTGGCTTTGAGAATGTTAGGAATGTTTATGAGTGGAGAGGTGTTAAACTTGAGGTTGATGAGACTAAGTATGATTTTG
Coverage
M13-Fwd TTTTAGGGTTTGTTTGTTTAGGTGGCTTTGAGAATGTTAGGAATGTTTATGAGTGGAGAGGTGTTAAACTTGAGGTTGATGAGACTAAGTATGATTTTG
Trace data
T7 TTTTAGGGTTTGTTTGTTTAGGTGGCTTTGAGAATGTTAGGAATGTTTATGAGTGGAGAGGTGTTAAACTTGAGGTTGATGAGACTAAGTATGATTTTG
Trace data
700
720
740
760
780
Transcript GGAATTGTTATGAGATTGAATGTGAGACAGAGGAACCAGAGCGTGTTAAGACAATGATTGAGGAGTTTCTTACAGAGGAGAAGATTGAGTTTTCGAATT
Consensus GGAATTGTTATGAGATTGAATGTGAGACAGAGGAACCAGAGCGTGTTAAGACAATGATTGAGGAGTTTCTTACAGAGGAGAAGATTGAGTTTTCGAATT
Coverage
M13-Fwd GGAATTGTTATGAGATTGAATGTGAGACAGAGGAACCAGAGCGTGTTAAGACAATGATTGAGGAGTTTCTTACAGAGGAGAAGATTGAGTTTTCGAATT
Trace data
T7 GGAATTGTTATGAGATTGAATGTGAGACAGAGGAACCAGAGCGTGTTAAGACAATGATTGAGGAGTTTCTTACAGAGGAGAAGATTGAGTTTTCGAATT
Trace data

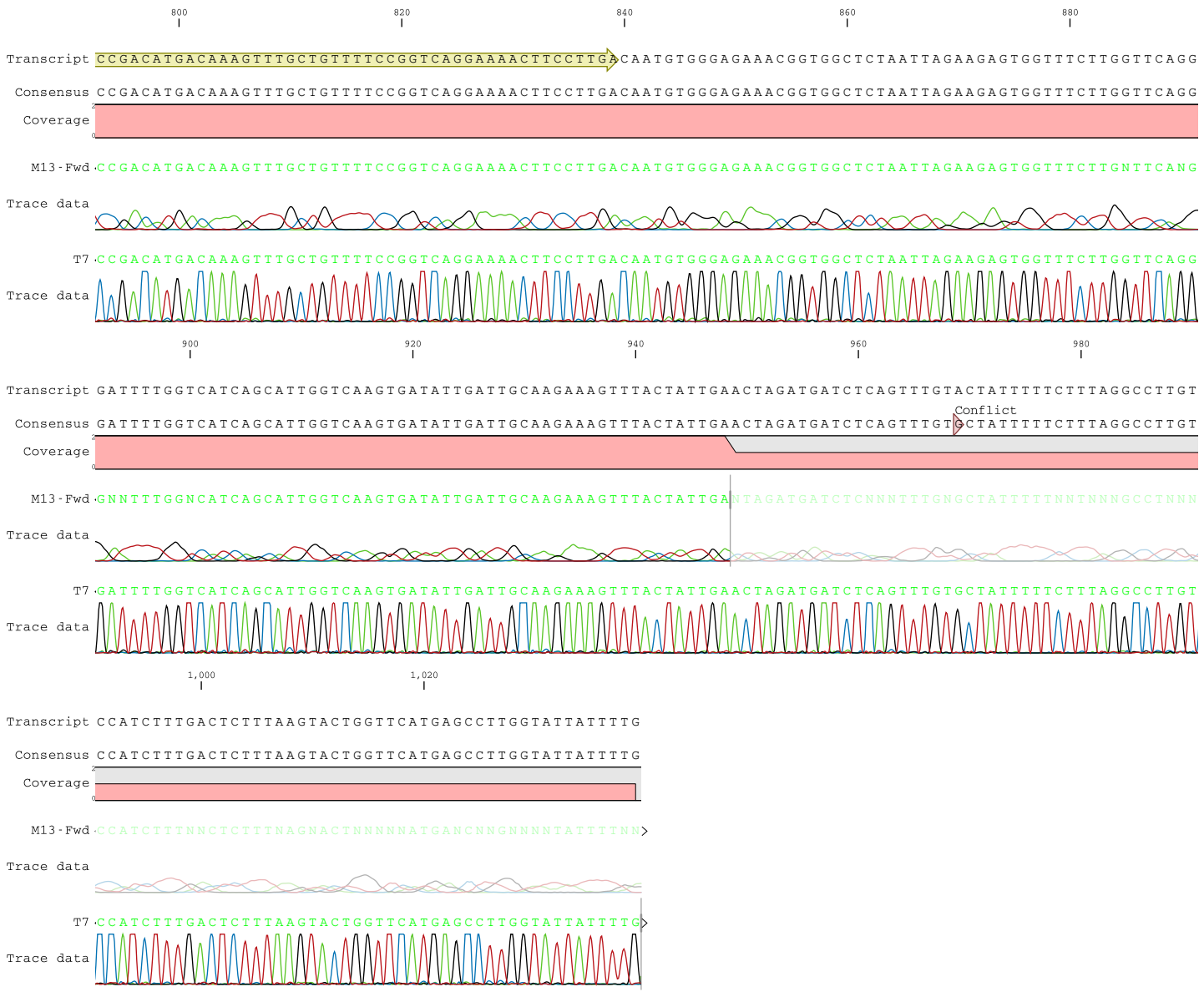
800
820
840
860
880
Transcript CCGACATGACAAAGTTTGCTGTTTTCCGGTCAGGAAAACTTCCTTGACAATGTGGGAGAAACGGTGGCTCTAATTAGAAGAGTGGTTTCTTGGTTCAGG
Consensus CCGACATGACAAAGTTTGCTGTTTTCCGGTCAGGAAAACTTCCTTGACAATGTGGGAGAAACGGTGGCTCTAATTAGAAGAGTGGTTTCTTGGTTCAGG
Coverage
M13-Fwd CCGACATGACAAAGTTTGCTGTTTTCCGGTCAGGAAAACTTCCTTGACAATGTGGGAGAAACGGTGGCTCTAATTAGAAGAGTGGTTTCTTGNTTCANG
Trace data
T7 CCGACATGACAAAGTTTGCTGTTTTCCGGTCAGGAAAACTTCCTTGACAATGTGGGAGAAACGGTGGCTCTAATTAGAAGAGTGGTTTCTTGGTTCAGG
Trace data
900
920
940
960
980
Transcript GATTTTGGTCATCAGCATTGGTCAAGTGATATTGATTGCAAGAAAGTTTACTATTGAACTAGATGATCTCAGTTTGTACTATTTTTCTTTAGGCCTTGT
Conflict
Consensus GATTTTGGTCATCAGCATTGGTCAAGTGATATTGATTGCAAGAAAGTTTACTATTGAACTAGATGATCTCAGTTTGTGCTATTTTTCTTTAGGCCTTGT
Coverage
M13-Fwd GNNTTTGGNCATCAGCATTGGTCAAGTGATATTGATTGCAAGAAAGTTTACTATTGANTAGATGATCTCNNNTTTGNGCTATTTTTNNTNNNGCCTNNN
Trace data
T7 GATTTTGGTCATCAGCATTGGTCAAGTGATATTGATTGCAAGAAAGTTTACTATTGAACTAGATGATCTCAGTTTGTGCTATTTTTCTTTAGGCCTTGT
Trace data
1,000
1,020
Transcript CCATCTTTGACTCTTTAAGTACTGGTTCATGAGCCTTGGTATTATTTTG
Consensus CCATCTTTGACTCTTTAAGTACTGGTTCATGAGCCTTGGTATTATTTTG
Coverage
M13-Fwd CCATCTTTNNCTCTTTNAGNACTNNNNNATGANCNNGNNNNTATTTTNN
Trace data
T7 CCATCTTTGACTCTTTAAGTACTGGTTCATGAGCCTTGGTATTATTTTG
Trace data

CDC26 shorter transcript

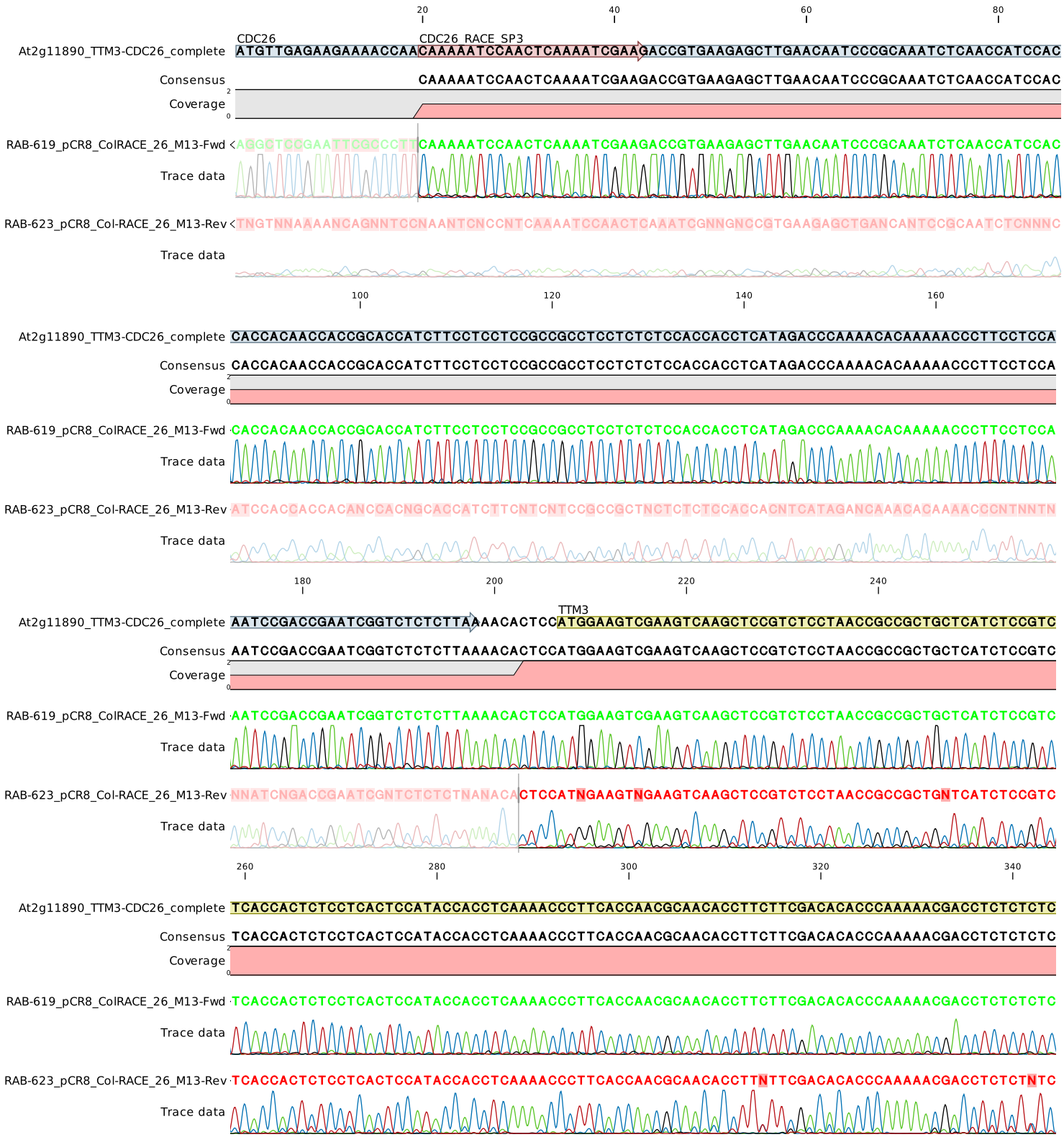

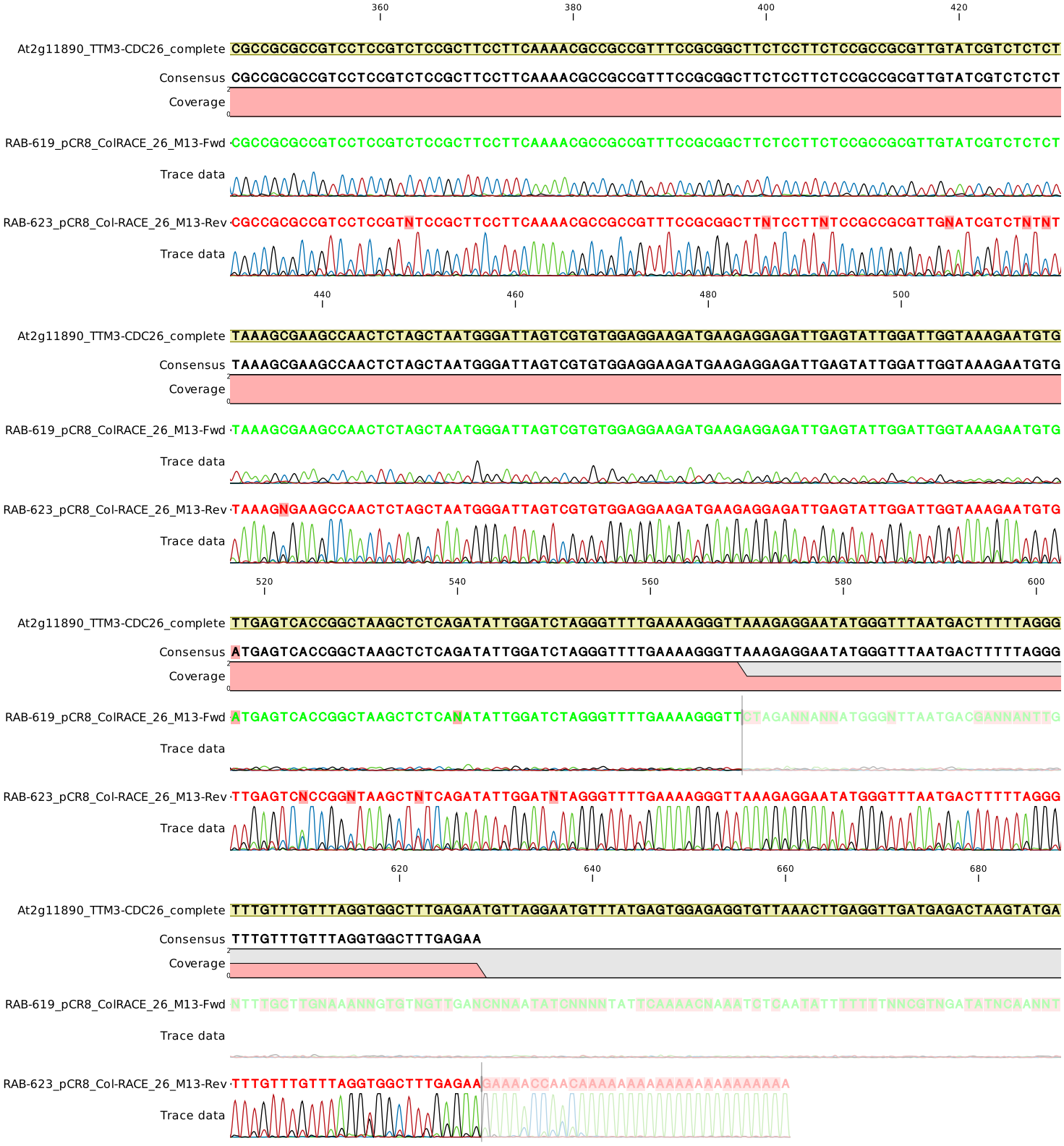
360
380
400
420
At2g11890_TTM3-CDC26_complete CGCCGCGCCGTCCTCCGTCTCCGCTTCCTTCAAAACGCCGCCGTTTCCGCGGCTTCTCCTTCTCCGCCGCGTTGTATCGTCTCTCT
Consensus CGCCGCGCCGTCCTCCGTCTCCGCTTCCTTCAAAACGCCGCCGTTTCCGCGGCTTCTCCTTCTCCGCCGCGTTGTATCGTCTCTCT
Coverage
RAB-619_pCR8_ColRACE_26_M13-Fwd CGCCGCGCCGTCCTCCGTCTCCGCTTCCTTCAAAACGCCGCCGTTTCCGCGGCTTCTCCTTCTCCGCCGCGTTGTATCGTCTCTCT
Trace data
RAB-623_pCR8_Col-RACE_26_M13-Rev CGCCGCGCCGTCCTCCGTNTCCGCTTCCTTCAAAACGCCGCCGTTTCCGCGGCTTNTCCTTNTCCGCCGCGTTGNATCGTCTNTNT
Trace data
440
460
480
500
At2g11890_TTM3-CDC26_complete TAAAGCGAAGCCAACTCTAGCTAATGGGATTAGTCGTGTGGAGGAAGATGAAGAGGAGATTGAGTATTGGATTGGTAAAGAATGTG
Consensus TAAAGCGAAGCCAACTCTAGCTAATGGGATTAGTCGTGTGGAGGAAGATGAAGAGGAGATTGAGTATTGGATTGGTAAAGAATGTG
Coverage
RAB-619_pCR8_ColRACE_26_M13-Fwd TAAAGCGAAGCCAACTCTAGCTAATGGGATTAGTCGTGTGGAGGAAGATGAAGAGGAGATTGAGTATTGGATTGGTAAAGAATGTG
Trace data
RAB-623_pCR8_Col-RACE_26_M13-Rev TAAAGNGAAGCCAACTCTAGCTAATGGGATTAGTCGTGTGGAGGAAGATGAAGAGGAGATTGAGTATTGGATTGGTAAAGAATGTG
Trace data
520
540
560
580
600
At2g11890_TTM3-CDC26_complete TTGAGTCACCGGCTAAGCTCTCAGATATTGGATCTAGGGTTTTGAAAAGGGTTAAAGAGGAATATGGGTTTAATGACTTTTTAGGG
Consensus ATGAGTCACCGGCTAAGCTCTCAGATATTGGATCTAGGGTTTTGAAAAGGGTTAAAGAGGAATATGGGTTTAATGACTTTTTAGGG
Coverage
RAB-619_pCR8_ColRACE_26_M13-Fwd ATGAGTCACCGGCTAAGCTCTCANATATTGGATCTAGGGTTTTGAAAAGGGTTCTAGANNANNATGGGNTTAATGACGANNANTTG
Trace data
RAB-623_pCR8_Col-RACE_26_M13-Rev TTGAGTCNCCGGNTAAGCTNTCAGATATTGGATNTAGGGTTTTGAAAAGGGTTAAAGAGGAATATGGGTTTAATGACTTTTTAGGG
Trace data
620
640
660
680
At2g11890_TTM3-CDC26_complete TTTGTTTGTTTAGGTGGCTTTGAGAATGTTAGGAATGTTTATGAGTGGAGAGGTGTTAAACTTGAGGTTGATGAGACTAAGTATGA
Consensus TTTGTTTGTTTAGGTGGCTTTGAGAA
Coverage
RAB-619_pCR8_ColRACE_26_M13-Fwd NTTTGCTTGNAAANNGTGTNGTTGANCNNAATATCNNNNTATTCAAAACNAAATGTGAATATTTTTTTNNCGTNGATATNCAANNT
Trace data
RAB-623_pCR8_Col-RACE_26_M13-Rev TTTGTTTGTTTAGGTGGCTTTGAGAAGAAAACCAACAAAAAAAAAAAAAAAAAAAAAAAA
Trace data


700
720
740
760
At2g11890_TTM3-CDC26_complete
TTTTGGGAATTGTTATGAGATTGAATGTGAGACAGAGGAACCAGAGCGTGTTAAGACAATGATTGAGGAGTTTCTTACAGAGGAGA
Consensus
Coverage
RAB-619_pCR8_ColRACE_26_M13-Fwd
GNAATTGANNN
Trace data
RAB-623_pCR8_Col-RACE_26_M13-Rev
Trace data
780
800
820
At2g11890_TTM3-CDC26_complete
AGATTGAGTTTTCGAATTCCGACATGACAAAGTTTGCTGTTTTCCGGTCAGGAAAACTTCCTTGA
Consensus
Coverage
RAB-619_pCR8_ColRACE_26_M13-Fwd
Trace data
RAB-623_pCR8_Col-RACE_26_M13-Rev
Trace data